Quantum transport in semiconductor-superconductor microjunctions
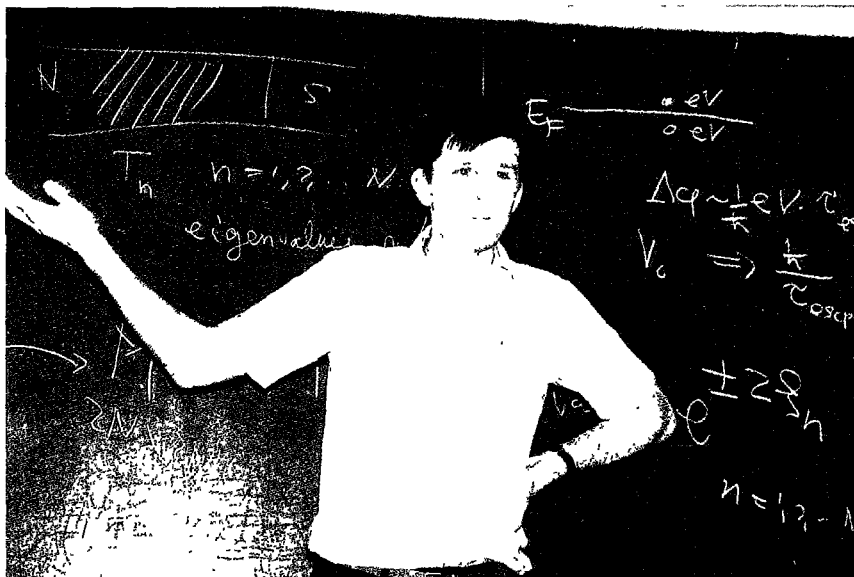Beenakker, C.W.J.

COURSE 5

QUANTUM TRANSPORT IN SEMICONDUCTOR–SUPERCONDUCTOR MICROJUNCTIONS

C.W.J. Beenakker

Instituut-Lorentz, University of Leiden
2300 RA Leiden, The Netherlands

Contents

1. Introduction

At the interface between a normal metal and a superconductor, dissipative electrical current is converted into dissipationless supercurrent. The mechanism for this conversion was discovered thirty years ago by A F Andreev [1]. An electron excitation slightly above the Fermi level in the normal metal is reflected at the interface as a hole excitation slightly below the Fermi level (see fig 1). The missing charge of $2e$ is removed as a supercurrent. The reflected hole has (approximately) the same momentum as the incident electron. (The two momenta are precisely equal at the Fermi level.) The velocity of the hole is minus the velocity of the electron (cf the notion of a hole as a "time-reversed" electron). This curious scattering process is known as retro-reflection or *Andreev reflection*.

The early theoretical work on the conductance of a normal-metal – superconductor (NS) junction treats the dynamics of the quasiparticle excitations *semiclassically*, as is appropriate for macroscopic junctions. Phase coherence of the electrons and the Andreev-reflected holes is ignored. Interest in "mesoscopic" NS junctions, where phase coherence plays an important role, is a recent development. Significant advances have been made during the last few years in our understanding of quantum interference effects due to phase-coherent Andreev reflection. Much of the motivation has come from the technological advances in the fabrication of a highly transparent contact between a superconducting film and the two-dimensional electron gas in a semiconductor heterostructure. These systems are ideal for the study of the interplay of Andreev reflection and the mesoscopic effects known to occur in semiconductor nanostructures [2], because of the large Fermi wavelength, large mean free path, and because of the possibility to confine the carriers electrostatically by means of gate electrodes. In this series of lectures we review the present status of this rapidly developing field of research.

To appreciate the importance of phase coherence in NS junctions, consider the resistance of a normal-metal wire (length L, mean free path l). This resistance increases monotonically with L. Now attach the wire to a superconductor via a tunnel barrier (transmission probability Γ). Then the resistance has a *minimum* when $L \simeq l/\Gamma$. The minimum disappears if the phase coherence between the electrons and holes is destroyed, by increasing the voltage or by applying a magnetic field. The resistance minimum is associated with the crossover from a Γ^{-1}
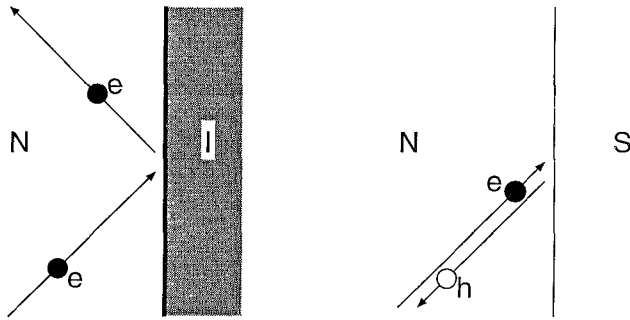
Fig 1 Normal reflection by an insulator (I) versus Andreev reflection by a superconductor (S) of an electron excitation in a normal metal (N) near the Fermi level Normal reflection (left) conserves charge but does not conserve momentum Andreev reflection (right) conserves momentum but does not conserve charge The electron (e) is reflected as a hole (h) with the same momentum and opposite velocity The missing charge of $2e$ is absorbed as a Cooper pair by the superconducting condensate

to a Γ^{-2} dependence on the barrier transparency The Γ^{-2} dependence is as expected for tunneling into a superconductor, being a two-particle process The Γ^{-1} dependence is surprising It is as if the Andreev-reflected hole can tunnel through the barrier without reflections This so called "reflectionless tunneling" requires relatively transparent NS interfaces, with $\Gamma \gtrsim l/L$ Semiconductor — superconductor junctions are convenient, since the Schottky barrier at the interface is much more transparent than a typical dielectric tunnel barrier The technological effort is directed towards making the interface as transparent as possible A nearly ideal NS interface ($\Gamma \simeq 1$) is required if one wishes to study how Andreev reflection modifies the quantum interference effects in the normal state (For $\Gamma \ll 1$ these are obscured by the much larger reflectionless-tunneling effect) The modifications can be quite remarkable We discuss two examples

The first is weak localization In the normal state, weak localization can not be detected in the current–voltage (I–V) characteristic, but requires application of a magnetic field The reason is that application of a voltage (in contrast to a magnetic field) does not break time-reversal symmetry In an NS junction, however, weak localization can be detected in the I–V characteristic, because application of a voltage destroys the phase coherence between electrons and holes The result is a small dip in $\partial I/\partial V$ versus V around $V = 0$ for $\Gamma \simeq 1$ On reducing Γ, the dip crosses over to a peak due to reflectionless tunneling The peak is much larger than the dip, but the widths are approximately the same

The second example is universal conductance fluctuations In the normal state, the conductance fluctuates from sample to sample with a variance which is independent of sample size or degree of disorder This is one aspect of the universality The other aspect is that breaking of time-reversal symmetry (by a magnetic field)

reduces the variance by precisely a factor of two In an NS junction, the conductance fluctuations are also size and disorder independent However, application of a time-reversal-symmetry breaking magnetic field has no effect on the magnitude

These three phenomena, weak localization, reflectionless tunneling, and universal conductance fluctuations, are discussed in sections 4, 5, and 6, respectively Sections 2 and 3 are devoted to a description of the theoretical method and to a few illustrative applications The method is a scattering theory, which relates the conductance G_{NS} of the NS junction to the $N \times N$ transmission matrix t in the normal state (N is the number of transverse modes at the Fermi level) In the limit of zero temperature, zero voltage, and zero magnetic field, the relationship is

$$G_{NS} = \frac{4e^2}{h} \sum_{n=1}^{N} \frac{T_n^2}{(2 - T_n)^2}, \tag{1 1}$$

where the transmission eigenvalue T_n is an eigenvalue of the matrix product $tt^\dagger$ The same numbers T_n ($n = 1, 2, \quad , N$) determine the conductance G_N in the normal state, according to the Landauer formula

$$G_N = \frac{2e^2}{h} \sum_{n=1}^{N} T_n \tag{1 2}$$

The fact that the same transmission eigenvalues determine both G_N and G_{NS} means that one can use the same (numerical and analytical) techniques developed for quantum transport in the normal state This is a substantial technical and conceptual simplification

The scattering theory can also be used for other transport properties, other than the conductance, both in the normal and the superconducting state An example, discussed in section 7, is the shot noise due to the discreteness of the carriers A doubling of the ratio of shot-noise power to current can occur in an NS junction, consistent with the notion of Cooper pair transport in the superconductor

We conclude in section 8

We restrict ourselves in this review (with one exception) to two-terminal geometries, with a single NS interface Equation (1 1), as well as the Landauer formula (1 2), only describe the two-terminal conductance More complex multiterminal geometries, involving several NS interfaces, have been studied theoretically by Lambert and coworkers [3,4], and experimentally by Petrashov et al [5] Since we focus on phase-coherent effects, most of our discussion concerns the linear-response regime of infinitesimal applied voltage A recent review by Klapwijk contains a more extensive coverage of the non-linear response at higher voltages [6] The scattering approach has also been applied to the Josephson effect in SNS junctions [7], resulting in a formula for the supercurrent–phase relation-

ship in terms of the transmission eigenvalues T_n in the normal state We do not
discuss the Josephson effect here, but refer to ref [8] for a review of mesoscopic
SNS junctions Taken together, ref [8] and the present work describe a unified
approach to mesoscopic superconductivity

2. Scattering theory

The model considered is illustrated in fig 2 It consists of a disordered normal re-
gion (hatched) adjacent to a superconductor (S) The disordered region may also
contain a geometrical constriction or a tunnel barrier To obtain a well-defined
scattering problem we insert ideal (impurity-free) normal leads N_1 and N_2 to the
left and right of the disordered region The NS interface is located at $x = 0$ We
assume that the only scattering in the superconductor consists of Andreev reflec-
tion at the NS interface, i e we consider the case that the disorder is contained
entirely within the normal region The spatial separation of Andreev and normal
scattering is the key simplification which allows us to relate the conductance dir-
ectly to the normal-state scattering matrix The model is directly applicable to
a superconductor in the clean limit (mean free path in S large compared to the
superconducting coherence length ξ), or to a point-contact junction (formed by
a constriction which is narrow compared to ξ) In both cases the contribution of
scattering within the superconductor to the junction resistance can be neglected
[9]

The scattering states at energy ε are eigenfunctions of the Bogoliubov–de
Gennes (BdG) equation This equation has the form of two Schrodinger equa-
tions for electron and hole wavefunctions $u(r)$ and $v(r)$, coupled by the pair
potential $\Delta(r)$ [10]

$$\left(\begin{array}{cc} \mathcal{H}_0 & \Delta \\ \Delta^* & -\mathcal{H}_0^* \end{array} \right) \left(\begin{array}{c} u \\ v \end{array} \right) = \varepsilon \left(\begin{array}{c} u \\ v \end{array} \right) \tag{2 1}$$
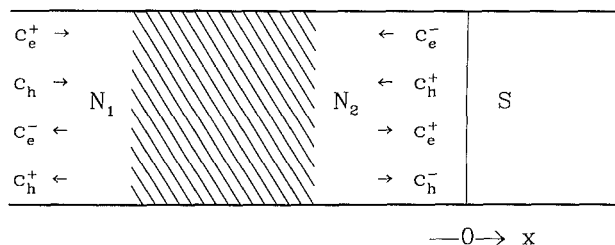

Fig 2   Normal metal–superconductor junction containing a disordered normal region (hatched)
Scattering states in the two normal leads N_1 and N_2 are indicated schematically

Here $\mathcal{H}_0 = (p + eA)^2/2m + V - E_\Gamma$ is the single-electron Hamiltonian, containing an electrostatic potential $V(r)$ and vector potential $A(r)$. The excitation energy ε is measured relative to the Fermi energy E_F. To simplify construction of the scattering basis we assume that the magnetic field B (in the z-direction) vanishes outside the disordered region. One can then choose a gauge such that $A \equiv 0$ in lead N_2 and in S, while $A_x, A_z = 0$, $A_y = A_1 \equiv$ constant in lead N_1.

The pair potential in the bulk of the superconductor ($x \gg \xi$) has amplitude Δ_0 and phase ϕ. The spatial dependence of $\Delta(r)$ near the NS interface is determined by the self-consistency relation [10]

$$\Delta(r) = |g(r)| \sum_{\varepsilon > 0} \mathrm{v}^*(r)\mathrm{u}(r)[1 - 2f(\varepsilon)], \tag{2 2}$$

where the sum is over all states with positive eigenvalue, and $f(\varepsilon) = [1 + \exp(\varepsilon/k_B T)]^{-1}$ is the Fermi function. The coefficient g is the interaction constant of the BCS theory of superconductivity. At an NS interface, g drops abruptly (over atomic distances) to zero, in the assumed absence of any pairing interaction in the normal region. Therefore, $\Delta(r) \equiv 0$ for $x < 0$. At the superconducting side of the NS interface, $\Delta(r)$ recovers its bulk value $\Delta_0 e^{i\phi}$ only at some distance from the interface. We will neglect the suppression of $\Delta(r)$ on approaching the NS interface, and use the step-function model

$$\Delta(r) = \Delta_0 e^{i\phi}\theta(x) \tag{2 3}$$

This model is also referred to in the literature as a "rigid boundary-condition". Likharev [11] discusses in detail the conditions for its validity. If the width W of the NS junction is small compared to ξ, the non-uniformities in $\Delta(r)$ extend only over a distance of order W from the junction (because of "geometrical dilution" of the influence of the narrow junction in the wide superconductor). Since non-uniformities on length scales $\ll \xi$ do not affect the dynamics of the quasiparticles, these can be neglected and the step-function model holds. A point contact or microbridge belongs in general to this class of junctions. Alternatively, the step-function model holds also for a wide junction if the resistivity of the junction region is much bigger than the resistivity of the bulk superconductor. This condition is formulated more precisely in ref [11]. A semiconductor — superconductor junction is typically in this second category. Note that both the two cases are consistent with our assumption that the disorder is contained entirely within the normal region.

It is worth emphasizing that the absence of a pairing interaction in the normal region ($g(r) \equiv 0$ for $x < 0$) implies a vanishing pair potential $\Delta(r)$, according to eq (2 2), but does not imply a vanishing order parameter $\Psi(r)$, which is given

by

$$\Psi(r) = \sum_{\varepsilon > 0} v^*(r) u(r)[1 - 2f(\varepsilon)] \tag{2 4}$$

Phase coherence between the electron and hole wave functions u and v leads to $\Psi(r) \neq 0$ for $x < 0$ The term "proximity effect" can therefore mean two different things One is the suppression of the pair potential Δ at the superconducting side of the NS interface This is a small effect which is neglected in the present work (and in most other papers in this field) The other is the induction of a non-zero order parameter Ψ at the normal side of the NS interface This effect is fully included here, even though Ψ does not appear explicitly in the expressions which follow The reason is that the order parameter quantifies the degree of phase coherence between electrons and holes, but does not itself affect the dynamics of the quasiparticles (The BdG equation (2 1) contains Δ not Ψ)

We now construct a basis for the scattering matrix (s matrix) In the normal lead N_2 the eigenfunctions of the BdG equation (2 1) can be written in the form

$$\psi_{n\,e}^{\pm}(N_2) = \begin{pmatrix} 1 \\ 0 \end{pmatrix} (k_n^e)^{-1/2} \, \Phi_n(y, z) \exp(\pm i k_n^e x),$$

$$\psi_{n\,h}^{\pm}(N_2) = \begin{pmatrix} 0 \\ 1 \end{pmatrix} (k_n^h)^{-1/2} \, \Phi_n(y, z) \exp(\pm i k_n^h x), \tag{2 5}$$

where the wavenumbers k_n^e and k_n^h are given by

$$k_n^{e\,h} \equiv (2m/\hbar^2)^{1/2}(E_F - E_n + \sigma^{e\,h}\varepsilon)^{1/2}, \tag{2 6}$$

and we have defined $\sigma^e \equiv 1$, $\sigma^h \equiv -1$ The labels e and h indicate the electron or hole character of the wavefunction The index n labels the modes, $\Phi_n(y, z)$ is the transverse wavefunction of the n-th mode, and E_n its threshold energy

$$[(p_y^2 + p_z^2)/2m + V(y, z)]\Phi_n(y, z) = E_n\Phi_n(y, z) \tag{2 7}$$

The eigenfunction Φ_n is normalized to unity, $\int dy \int dz\, |\Phi_n|^2 = 1$ With this normalization each wavefunction in the basis (2 5) carries the same amount of quasiparticle current The eigenfunctions in lead N_1 are chosen similarly, but with an additional phase factor $\exp[-i\sigma^{e\,h}(eA_1/\hbar)y]$ from the vector potential

A wave incident on the disordered normal region is described in the basis (2 5) by a vector of coefficients

$$c_N^{in} \equiv \left(c_e^+(N_1), c_e^-(N_2), c_h^-(N_1), c_h^+(N_2)\right) \tag{2 8}$$

(The mode-index n has been suppressed for simplicity of notation) The reflected and transmitted wave has vector of coefficients

$$c_N^{out} \equiv \left(c_e^-(N_1), c_e^+(N_2), c_h^+(N_1), c_h^-(N_2)\right) \tag{2 9}$$

The s-matrix s_N of the normal region relates these two vectors,

$$c_N^{\text{out}} = s_N c_N^{\text{in}} \tag{2 10}$$

Because the normal region does not couple electrons and holes, this matrix has the block-diagonal form

$$s_N(\varepsilon) = \begin{pmatrix} s_0(\varepsilon) & 0 \\ 0 & s_0(-\varepsilon)^* \end{pmatrix}, \; s_0 \equiv \begin{pmatrix} r_{11} & t_{12} \\ t_{21} & r_{22} \end{pmatrix} \tag{2 11}$$

Here s_0 is the unitary s-matrix associated with the single-electron Hamiltonian $\mathcal{H}_0$ The reflection and transmission matrices $r(\varepsilon)$ and $t(\varepsilon)$ are $N \times N$ matrices, $N(\varepsilon)$ being the number of propagating modes at energy ε (We assume for simplicity that the number of modes in leads N_1 and N_2 is the same) The matrix s_0 is unitary ($s_0^\dagger s_0 = 1$) and satisfies the symmetry relation $s_0(\varepsilon, B)_{ij} = s_0(\varepsilon, -B)_{ji}$

For energies $0 < \varepsilon < \Delta_0$ there are no propagating modes in the superconductor We can then define an s-matrix for Andreev reflection at the NS interface which relates the vector of coefficients $\left(c_e^-(N_2), c_h^+(N_2)\right)$ to $\left(c_e^+(N_2), c_h^-(N_2)\right)$ The elements of this s-matrix can be obtained by matching the wavefunctions (2 5) at $x = 0$ to the decaying solutions in S of the BdG equation If terms of order Δ_0/E_F are neglected (the so called Andreev approximation [1]), the result is simply

$$c_e^-(N_2) = \alpha\, e^{i\phi} c_h^-(N_2),$$
$$c_h^+(N_2) = \alpha\, e^{-i\phi} c_e^+(N_2), \tag{2 12}$$

where $\alpha \equiv \exp[-i\arccos(\varepsilon/\Delta_0)]$ Andreev reflection transforms an electron mode into a hole mode, without change of mode index The transformation is accompanied by a phase shift, which consists of two parts

(i) A phase shift $-\arccos(\varepsilon/\Delta_0)$ due to the penetration of the wavefunction into the superconductor

(ii) A phase shift equal to plus or minus the phase of the pair potential in the superconductor (*plus* for reflection from hole to electron, *minus* for the reverse process)

We can combine the $2N$ linear relations (2 12) with the $4N$ relations (2 10) to obtain a set of $2N$ linear relations between the incident wave in lead N_1 and the reflected wave in the same lead

$$c_e^-(N_1) = s_{ee} c_e^+(N_1) + s_{eh} c_h^-(N_1),$$
$$c_h^+(N_1) = s_{he} c_e^+(N_1) + s_{hh} c_h^-(N_1) \tag{2 13}$$

The four $N \times N$ matrices s_{ee}, s_{hh}, s_{eh}, and s_{he} form together the scattering matrix s of the whole system for energies $0 < \varepsilon < \Delta_0$ An electron incident in lead N_1 is reflected either as an electron (with scattering amplitudes s_{ee}) or as a

hole (with scattering amplitudes s_{he}) Similarly, the matrices s_{hh} and s_{eh} contain the scattering amplitudes for reflection of a hole as a hole or as an electron After some algebra we find for these matrices the expressions

$$s_{ee}(\varepsilon) = r_{11}(\varepsilon) + \alpha^2 t_{12}(\varepsilon) r_{22}^*(-\varepsilon) M_e t_{21}(\varepsilon), \qquad (2\ 14)$$

$$s_{hh}(\varepsilon) = r_{11}^*(-\varepsilon) + \alpha^2 t_{12}^*(-\varepsilon) r_{22}(\varepsilon) M_h t_{21}^*(-\varepsilon), \qquad (2\ 15)$$

$$s_{eh}(\varepsilon) = \alpha\, e^{i\phi} t_{12}(\varepsilon) M_h t_{21}^*(-\varepsilon), \qquad (2\ 16)$$

$$s_{he}(\varepsilon) = \alpha\, e^{-i\phi} t_{12}^*(-\varepsilon) M_e t_{21}(\varepsilon), \qquad (2\ 17)$$

where we have defined the matrices

$$M_e \equiv [1 - \alpha^2 r_{22}(\varepsilon) r_{22}^*(-\varepsilon)]^{-1},$$

$$M_h \equiv [1 - \alpha^2 r_{22}^*(-\varepsilon) r_{22}(\varepsilon)]^{-1} \qquad (2\ 18)$$

One can verify that the s-matrix constructed from these four sub-matrices satisfies unitarity ($s^\dagger s = 1$) and the symmetry relation $s(\varepsilon, B, \phi)_{ij} = s(\varepsilon, -B, -\phi)_{ji}$, as required by quasiparticle-current conservation and by time-reversal invariance, respectively

For the linear-response conductance G_{NS} of the NS junction at zero temperature we only need the s-matrix at the Fermi level, i e at $\varepsilon = 0$ We restrict ourselves to this case and omit the argument ε in what follows We apply the general formula [12–14]

$$G_{NS} = \frac{2e^2}{h}\mathrm{Tr}\,(1 - s_{ee}s_{ee}^\dagger + s_{he}s_{he}^\dagger) = \frac{4e^2}{h}\mathrm{Tr}\,s_{he}s_{he}^\dagger \qquad (2\ 19)$$

The second equality follows from unitarity of s, which implies $1 - s_{ee}s_{ee}^\dagger = s_{eh}s_{eh}^\dagger = (s_{ee}^\dagger)^{-1}s_{he}^\dagger s_{he}s_{ee}^\dagger$, so that $\mathrm{Tr}\,(1 - s_{ee}s_{ee}^\dagger) = \mathrm{Tr}\,s_{he}s_{he}^\dagger$ We now substitute eq (2 17) for $\varepsilon = 0$ ($\alpha = -1$) into eq (2 19), and obtain the expression

$$G_{NS} = \frac{4e^2}{h}\mathrm{Tr}\,t_{12}^\dagger t_{12}(1 + r_{22}^* r_{22})^{-1} t_{21}^\dagger t_{21}^T (1 + r_{22}^\dagger r_{22}^T)^{-1}, \qquad (2\ 20)$$

where $M^T \equiv (M^*)^\dagger$ denotes the transpose of a matrix The advantage of eq (2 20) over eq (2 19) is that the former can be evaluated by using standard techniques developed for quantum transport in the normal state, since the only input is the normal-state scattering matrix The effects of multiple Andreev reflections are fully incorporated by the two matrix inversions in eq (2 20)

In the absence of a magnetic field the general formula (2 20) simplifies considerably Since the s-matrix s_0 of the normal region is symmetric for $B = 0$, one has $r_{22} = r_{22}^T$ and $t_{12} = t_{21}^T$ Equation (2 20) then takes the form

$$G_{NS} = \frac{4e^2}{h}\mathrm{Tr}\,t_{12}^\dagger t_{12}(1 + r_{22}^\dagger r_{22})^{-1} t_{12}^\dagger t_{12}(1 + r_{22}^\dagger r_{22})^{-1}$$

$$= \frac{4e^2}{h} \mathrm{Tr} \left(t_{12}^\dagger t_{12} (2 - t_{12}^\dagger t_{12})^{-1} \right)^2 \tag{2 21}$$

In the second equality we have used the unitarity relation $r_{22}^\dagger r_{22} + t_{12}^\dagger t_{12} = 1$ The trace (2 21) depends only on the eigenvalues of the Hermitian matrix $t_{12}^\dagger t_{12}$ We denote these eigenvalues by T_n ($n = 1, 2,\ \ N$) Since the matrices $t_{12}^\dagger t_{12}, t_{12} t_{12}^\dagger, t_{21}^\dagger t_{21}$, and $t_{21} t_{21}^\dagger$ all have the same set of eigenvalues, we can omit the indices and write simply $tt^\dagger$ We obtain the following relation between the conductance and the transmission eigenvalues

$$G_{\mathrm{NS}} = \frac{4e^2}{h} \sum_{n=1}^{N} \frac{T_n^2}{(2 - T_n)^2} \tag{2 22}$$

This is the central result of ref [15]

Equation (2 22) holds for an arbitrary transmission matrix t, i e for arbitrary disorder potential It is the *multi-channel* generalization of a formula first obtained by Blonder, Tinkham, and Klapwijk [12] (and subsequently by Shelankov [16] and by Zaïtsev [17]) for the *single channel* case (appropriate for a geometry such as a planar tunnel barrier, where the different scattering channels are uncoupled) A formula of similar generality for the normal-metal conductance G_N is the multi-channel Landauer formula

$$G_\mathrm{N} = \frac{2e^2}{h} \mathrm{Tr}\, tt^\dagger \equiv \frac{2e^2}{h} \sum_{n=1}^{N} T_n \tag{2 23}$$

In contrast to the Landauer formula, eq (2 22) for the conductance of an NS junction is a *non linear* function of the transmission eigenvalues T_n When dealing with a non-linear multi channel formula as eq (2 22), it is of importance to distinguish between the transmission eigenvalue T_n and the modal transmission probability $\mathcal{T}_n \equiv \sum_{m=1}^{N} |t_{nm}|^2$ The former is an eigenvalue of the matrix $tt^\dagger$, the latter a diagonal element of that matrix The Landauer formula (2 23) can be written equivalently as a sum over eigenvalues or as sum over modal transmission probabilities

$$\frac{h}{2e^2} G_\mathrm{N} = \sum_{n=1}^{N} T_n \equiv \sum_{n=1}^{N} \mathcal{T}_n \tag{2 24}$$

This equivalence is of importance for (numerical) evaluations of the Landauer formula, in which one calculates the probability that an electron injected in mode n is transmitted, and then obtains the conductance by summing over all modes The non-linear scattering formula (2 22), in contrast, can not be written in terms of modal transmission probabilities alone The off-diagonal elements of $tt^\dagger$ contribute to G_{NS} in an essential way Previous attempts to generalize the one-

dimensional Blonder–Tinkham–Klapwijk formula to more dimensions by summing over modal transmission probabilities (or, equivalently, by angular averaging) were not successful precisely because only the diagonal elements of $tt^\dagger$ were considered

3. Three simple applications

To illustrate the power and generality of the scattering formula (2 22), we discuss in this section three simple applications to the ballistic, resonant-tunneling, and diffusive transport regimes [15]

3 1   Quantum point contact

Consider first the case that the normal metal consists of a ballistic constriction with a normal-state conductance quantized at $G_N = 2N_0 e^2/h$ (a *quantum point contact*)   The integer N_0 is the number of occupied one-dimensional subbands (per spin direction) in the constriction, or alternatively the number of transverse modes at the Fermi level which can propagate through the constriction   Note that $N_0 \ll N$ An "ideal" quantum point contact is characterized by a special set of transmission eigenvalues, which are equal to either zero or one [2]

$$T_n = \begin{cases} 1 & \text{if } 1 \le n \le N_0, \\ 0 & \text{if } N_0 < n \le N, \end{cases} \tag{3 1}$$

where the eigenvalues have been ordered from large to small   We emphasize that eq (3 1) does not imply that the transport through the constriction is adiabatic   In the case of adiabatic transport, the transmission eigenvalue T_n is equal to the modal transmission probability $\mathcal{T}_n$ In the absence of adiabaticity there is no direct relation between T_n and $\mathcal{T}_n$ Substitution of eq (3 1) into eq (2 22) yields

$$G_{NS} = \frac{4e^2}{h} N_0 \tag{3 2}$$

The conductance of the NS junction is quantized in units of $4e^2/h$ This is *twice* the conductance quantum in the normal state, due to the current-doubling effect of Andreev reflection [18]

In the classical limit $N_0 \to \infty$ we recover the well known result $G_{NS} = 2G_N$ for a *classical* ballistic point contact [12,16,19]   In the quantum regime, however, the simple factor-of-two enhancement only holds for the conductance plateaus, where eq (3 1) applies, and not to the transition region between two subsequent plateaus of quantized conductance   To illustrate this, we compare in fig 3 the conductances G_{NS} and $2G_N$ for Buttiker's model [20] of a saddle-point constriction in a two-dimensional electron gas   Appreciable differences appear in the
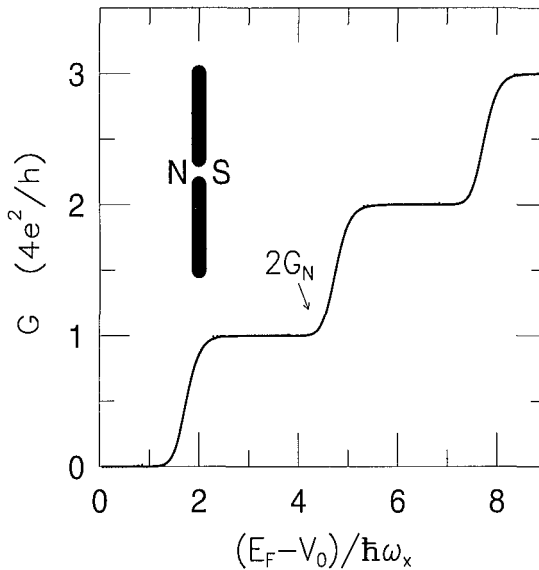
Fig 3 Solid curve Conductance G_{NS} versus Fermi energy of a quantum point contact between a normal and a superconducting reservoir (shown schematically in the inset) The dotted curve is twice the conductance G_N for the case of two normal reservoirs [20] The constriction is defined by the 2D saddle point potential $V(x\ y) = V_0 - \frac{1}{2}m\omega_x^2 x^2 + \frac{1}{2}m\omega_y^2 y^2$ with $\omega_y/\omega_x = 3$ G_{NS} is calculated from eq (2 22) with $T_n = [1 + \exp(-2\pi\varepsilon_n/\hbar\omega_x)]^{-1}$ $\varepsilon_n \equiv E_F - V_0 - (n - \frac{1}{2})\hbar\omega_y$ (From ref [15])

transition region, where G_{NS} lies below twice G_N This is actually a rigorous inequality, which follows from eqs (2 22) and (2 23) for *arbitrary* transmission matrix

$$G_{NS} \leq 2G_N, \ \forall t \tag{3 3}$$

3 2 Quantum dot

Consider next a small confined region (of dimensions comparable to the Fermi wavelength), which is weakly coupled by tunnel barriers to two electron reservoirs We assume that transport through this *quantum dot* occurs via resonant tunneling through a single bound state Let ε_{res} be the energy of the resonant level, relative to the Fermi level in the reservoirs, and let $\gamma_1/\hbar$ and $\gamma_2/\hbar$ be the tunnel rates through the two barriers We denote $\gamma \equiv \gamma_1 + \gamma_2$ If $\gamma \ll \Delta E$ (with ΔE the level spacing in the quantum dot), the conductance G_N in the case of
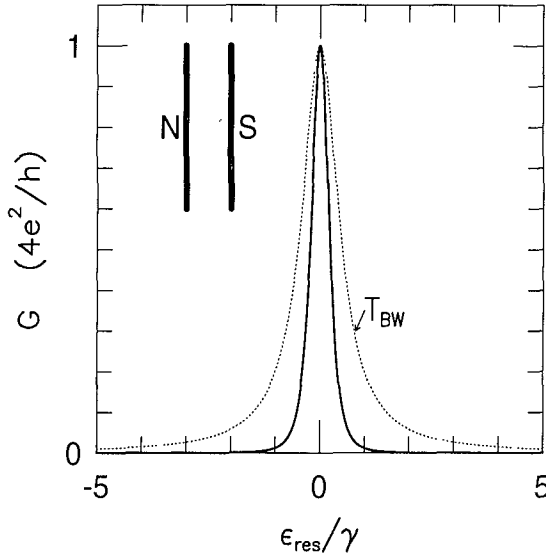
Fig. 4. Conductance versus energy of the resonant level, from eq. (3.8) for the case of equal tunnel barriers (solid curve). The dotted curve is the Breit–Wigner transmission probability (3.4). The inset shows schematically the normal-metal — quantum-dot — superconductor junction.

non-interacting electrons has the form

$$\frac{h}{2e^2}G_N = \frac{\gamma_1\gamma_2}{\varepsilon_{res}^2 + \frac{1}{4}\gamma^2} \equiv T_{BW}, \tag{3.4}$$

with T_{BW} the Breit–Wigner transmission probability at the Fermi level. The normal-state transmission matrix $t_{12}(\varepsilon)$ which yields this conductance has matrix elements [21]

$$t_{12}(\varepsilon) = U_1\tau(\varepsilon)U_2, \quad \tau(\varepsilon)_{nm} \equiv \frac{\sqrt{\gamma_{1n}\gamma_{2m}}}{\varepsilon - \varepsilon_{res} + \frac{1}{2}i\gamma}, \tag{3.5}$$

where $\sum_n \gamma_{1n} \equiv \gamma_1$, $\sum_n \gamma_{2n} \equiv \gamma_2$, and U_1, U_2 are two unitary matrices (which need not be further specified).

Let us now investigate how the conductance (3.4) is modified if one of the two reservoirs is in the superconducting state. The transmission matrix product $t_{12}t_{12}^\dagger$ (evaluated at the Fermi level $\varepsilon = 0$) following from eq. (3.5) is

$$t_{12}t_{12}^\dagger = U_1 M U_1^\dagger, \quad M_{nm} \equiv \frac{T_{BW}}{\gamma_1}\sqrt{\gamma_{1n}\gamma_{1m}}. \tag{3.6}$$

Its eigenvalues are

$$T_n = \begin{cases} T_{\text{BW}} & \text{if } n = 1, \\ 0 & \text{if } 2 \le n \le N \end{cases} \tag{3 7}$$

Substitution into eq (2 22) yields the conductance

$$G_{\text{NS}} = \frac{4e^2}{h} \left(\frac{T_{\text{BW}}}{2 - T_{\text{BW}}} \right)^2 = \frac{4e^2}{h} \left(\frac{2\gamma_1 \gamma_2}{4\varepsilon_{\text{res}}^2 + \gamma_1^2 + \gamma_2^2} \right)^2 \tag{3 8}$$

The conductance on resonance ($\varepsilon_{\text{res}} = 0$) is maximal in the case of equal tunnel rates ($\gamma_1 = \gamma_2$), and is then equal to $4e^2/h$ — independent of γ The lineshape for this case is shown in fig 4 (solid curve) It differs substantially from the Lorentzian lineshape (3 4) of the Breit–Wigner formula (dotted curve)

The amplitude and lineshape of the conductance resonance (3 8) does not depend on the relative magnitude of the resonance width γ and the superconducting energy gap Δ_0 This is in contrast to the supercurrent resonance in a superconductor — quantum dot — superconductor Josephson junction, which depends sensitively on the ratio γ/Δ_0 [22,23] The difference can be traced to the fact that the conductance (in the zero-temperature, zero-voltage limit) is strictly a Fermi-level property, whereas all states within Δ_0 of the Fermi level contribute to the Josephson effect (For an extension of eq (3 8) to finite voltages, see ref [24]) Since we have assumed non-interacting quasiparticles, the above results apply to a quantum dot with a small charging energy U for double occupancy of the resonant state Devyatov and Kupriyanov [25], and Hekking et al [26], have studied the influence of Coulomb repulsion on resonant tunneling through an NS junction, in the temperature regime $k_B T \gg \gamma$ where the resonance is thermally broadened The extension to the low-temperature regime of an intrinsically broadened resonance remains to be investigated

3 3 Disordered junction

We now turn to the regime of diffusive transport through a disordered point contact or microbridge between a normal and a superconducting reservoir The model considered is that of an NS junction containing a disordered normal region of length L much greater than the mean free path l for elastic impurity scattering, but much smaller than the localization length Nl We calculate the average conductance of the junction, averaged over an ensemble of impurity configurations We begin by parameterizing the transmission eigenvalue T_n in terms of a channel-dependent localization length ζ_n

$$T_n = \frac{1}{\cosh^2(L/\zeta_n)} \tag{3 9}$$

A fundamental result in quantum transport is that the inverse localization length is *uniformly* distributed between 0 and $1/\zeta_{min} \simeq 1/l$ for $l \ll L \ll Nl$ [27–30] One can therefore write

$$\frac{\left\langle \sum_{n=1}^{N} f(T_n) \right\rangle}{\left\langle \sum_{n=1}^{N} T_n \right\rangle} = \frac{\int_0^{L/\zeta_{min}} dx\, f(\cosh^{-2} x)}{\int_0^{L/\zeta_{min}} dx\, \cosh^{-2} x} = \int_0^{\infty} dx\, f(\cosh^{-2} x),$$

(3 10)

where $\langle \quad \rangle$ indicates the ensemble average and $f(T)$ is an arbitrary function of the transmission eigenvalue such that $f(T) \to 0$ for $T \to 0$ In the second equality in eq (3 10) we have used that $L/\zeta_{min} \simeq L/l \gg 1$ to replace the upper integration limit by ∞

Combining eqs (2 22), (2 23), and (3 10), we find

$$\langle G_{NS} \rangle = 2\langle G_N \rangle \int_0^{\infty} dx \left(\frac{\cosh^{-2} x}{2 - \cosh^{-2} x} \right)^2 = \langle G_N \rangle$$

(3 11)

We conclude that — although G_{NS} according to eq (2 22) is of *second* order in the transmission eigenvalues T_n — the ensemble average $\langle G_{NS} \rangle$ is of *first* order in l/L The resolution of this paradox is that the T's are not distributed uniformly, but are either exponentially small (closed channels) or of order unity (open channels) [28] Hence the average of T_n^2 is of the same order as the average of T_n Off-diagonal elements of the transmission matrix $tt^{\dagger}$ are crucial to arrive at the result (3 11) Indeed, if one would evaluate eq $\cdot$(2 22) with the transmission eigenvalues T_n replaced by the modal transmission probabilities $\mathcal{T}_n$, one would find a totally wrong result Since $\mathcal{T}_n \simeq l/L \ll 1$, one would find $G_{NS} \simeq (l/L)G_N$ — which underestimates the conductance of the NS junction by the factor L/l

Previous work [31,32] had obtained the equality of G_{NS} and G_N from *semi-classical* equations of motion, as was appropriate for macroscopic systems which are large compared to the normal-metal phase-coherence length l_{ϕ} The present derivation, in contrast, is fully quantum mechanical It applies to the "mesoscopic" regime $L < l_{\phi}$, in which transport is phase coherent Takane and Ebisawa [33] have studied the conductance of a disordered phase-coherent NS junction by numerical simulation of a two-dimensional tight-binding model They found $\langle G_{NS} \rangle = \langle G_N \rangle$ within numerical accuracy for $l \ll L \ll Nl$, in agreement with eq (3 11)

If the condition $L \ll Nl$ is relaxed, differences between $\langle G_{NS} \rangle$ and $\langle G_N \rangle$ appear To lowest order in L/Nl, the difference is a manifestation of the *weak-localization* effect, as we discuss in the following section

4. Weak localization

An NS junction shows an *enhanced* weak-localization effect, in comparison with the normal state [15] The origin of the enhancement can be understood in a simple way, as follows

We return to the parameterization $T_n \equiv 1/\cosh^2(L/\zeta_n)$ introduced in eq (3 9), and define the density of localization lengths $\rho(\zeta, L) \equiv \langle \sum_n \delta(\zeta - \zeta_n) \rangle_L$ The subscript L refers to the length of the disordered region Using the identity $\cosh 2x = 2\cosh^2 x - 1$, the ensemble-average of eq (2 22) becomes

$$\langle G_{\mathrm{NS}} \rangle_L = \frac{4e^2}{h} \int_0^\infty \mathrm{d}\zeta\, \rho(\zeta, L) \cosh^{-2}(2L/\zeta) \tag{4 1}$$

In the same parameterization, one has

$$\langle G_{\mathrm{N}} \rangle_L = \frac{2e^2}{h} \int_0^\infty \mathrm{d}\zeta\, \rho(\zeta, L) \cosh^{-2}(L/\zeta) \tag{4 2}$$

In the "open-channel approximation" [34], the integrals over ζ are restricted to the range $\zeta > L$ of localization lengths greater than the length of the conductor In this range the density $\rho(\zeta, L)$ is approximately independent of L The whole L-dependence of the integrands in eqs (4 1) and (4 2) lies then in the argument of the hyperbolic cosine, so that

$$\langle G_{\mathrm{NS}} \rangle_L = 2 \langle G_{\mathrm{N}} \rangle_{2L} \tag{4 3}$$

This derivation formalizes the intuitive notion that Andreev reflection at an NS interface effectively doubles the length of the normal-metal conductor [33]

Consider now the geometry $W \ll L$ relevant for a microbridge In the normal state one has

$$\langle G_{\mathrm{N}} \rangle = (W/L)\sigma_{\mathrm{Drude}} - \delta G_{\mathrm{N}}, \tag{4 4}$$

where σ_{Drude} is the classical Drude conductivity The L-independent term δG_{N} is the weak-localization correction, given by [35] $\delta G_N = \frac{2}{3}\, e^2/h$ Equation (4 3) then implies that

$$\langle G_{\mathrm{NS}} \rangle = (W/L)\sigma_{\mathrm{Drude}} - \delta G_{\mathrm{NS}}, \tag{4 5}$$

with $\delta G_{\mathrm{NS}} = 2\,\delta G_{\mathrm{N}}$ We conclude that Andreev reflection increases the weak-localization correction, by a factor of two according to this qualitative argument [15] A rigorous theory [36–38] of weak localization in an NS microbridge shows that the increase is actually somewhat less than a factor of two,*

$$\delta G_{\mathrm{NS}} = (2 - 8\pi^{-2})\, e^2/h = 1\ 78\, \delta G_{\mathrm{N}} \tag{4 6}$$

* Equation (4 6) follows from the general formula $\delta A = \frac{1}{4}a(1) + \int_0^\infty \mathrm{d}x\,(4x^2 + \pi^2)^{-1}a(\cosh^{-2}x)$ for the weak localization correction in a wire geometry where A is an arbitrary transport property of the form $A = \sum_n a(T_n)$

As pointed out in ref [39], the enhancement of weak localization in an NS junction can be observed experimentally as a *dip* in the differential conductance $G_{NS}(V) = \partial I/\partial V$ around zero voltage. The dip occurs because an applied voltage destroys the enhancement of weak localization by Andreev reflection, thereby increasing the conductance by an amount

$$\delta G_{NS} - \delta G_N \approx 0\ 5\,e^2/h \tag{4 7}$$

at zero temperature. [At finite temperatures, we expect a reduction of the size of dip by a factor* $(L_c/L)^2$, where $L_c = \min(l_\phi, \sqrt{\hbar D/k_B T})$ is the length over which electrons and holes remain phase coherent.] We emphasize that in the normal state, weak localization can *not* be detected in the current–voltage characteristic. The reason why a dip occurs in $G_{NS}(V)$ and not in $G_N(V)$ is that an applied voltage (in contrast to a magnetic field) does not break time-reversal symmetry — but only affects the phase coherence between the electrons and the Andreev-reflected holes (which differ in energy by up to $2eV$). The width V_c of the conductance dip is of the order of the Thouless energy $E_c \equiv \pi\hbar D/L^2$ (with D the diffusion coefficient of the junction, L should be replaced by L_c if $L > L_c$). This energy scale is such that an electron and a hole acquire a phase difference of order π on traversing the junction. The energy E_c is much smaller than the superconducting energy gap Δ_0, provided $L \gg \xi$ (with $\xi \simeq (\hbar D/\Delta_0)^{1/2}$ the superconducting coherence length in the dirty-metal limit). The separation of energy scales is important, in order to be able to distinguish experimentally the current due to Andreev reflection below the energy gap from the quasi-particle current above the energy gap.

The first measurement of the conductance dip predicted in ref [39] has been reported recently by Lenssen et al [40]. The system studied consists of the two-dimensional electron gas in a GaAs/AlGaAs heterostructure with Sn/Ti superconducting contacts ($W = 10\,\mu m$, $L = 0\ 8\,\mu m$). No supercurrent is observed, presumably because $l_\phi \simeq 0\ 4\,\mu m$ is smaller than L. (The phase-coherence length l_ϕ is estimated from a conventional weak-localization measurement in a magnetic field.) The data for the differential conductance is reproduced in fig 5. At the lowest temperatures (10 mK) a rather small and narrow conductance dip develops, superimposed on a large and broad conductance minimum. The size of the conductance dip is about $2\,e^2/h$. Since in the experimental geometry $W > L > l_\phi$, and there are two NS interfaces, we would expect a dip of or-

---

* The reduction factor $(L_c/L)^2$ for the size of the conductance dip when $W < L_c < L$ is estimated as follows. Consider the wire as consisting of L/L_c phase-coherent segments of length L_c in series. The first segment, adjacent to the superconductor, has a conductance dip $\delta G_1 \simeq e^2/h$, while the other segments have no conductance dip. The resistance R_1 of a single segment is a fraction L_c/L of the total resistance R of the wire. Since $\delta G/G = -\delta R/R = -\delta R_1/R$ and $\delta R_1 = -R_1^2 \delta G_1 \simeq -(L_c/L)^2 R^2 e^2/h$ we find $\delta G \simeq (L_c/L)^2 e^2/h$.
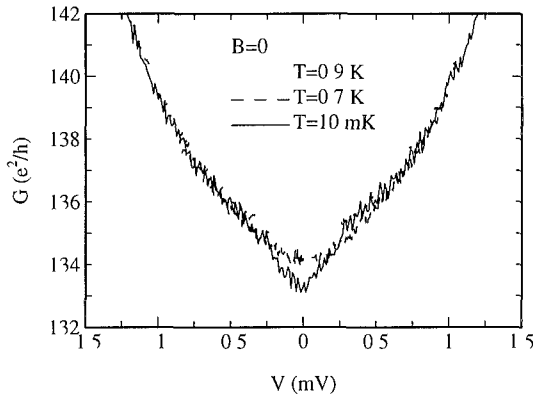
Fig 5   Differential conductance as a function of applied voltage at three different temperatures Experimental data by Lenssen et al for a two dimensional election gas with superconducting contacts The dip around zero voltage which is superimposed on the broad minimum at the lowest temperature is attributed to the enhancement of weak localization by Andreev reflection (From ref [40])

der $2(W/l_\phi)(l_\phi/L)^2 \times 0\,5\,e^2/h \simeq 6\,e^2/h$, simply by counting the number of phase coherent segments adjacent to the superconductor This is three times as large as observed, but the presence of a tunnel barrier at the NS interface might easily account for this discrepancy (The Schottky barrier at the interface between a semiconductor and superconductor presents a natural origin for such a barrier) The conductance dip has width $V_c \simeq 0\,25\,\mathrm{mV}$, which is less than the energy gap $\Delta_o = 0\,56\,\mathrm{meV}$ of bulk Sn — but not by much Experiments with a larger separation of energy scales are required for a completely unambiguous identification of the phenomenon

An essential requirement for the appearance of a dip in the differential conductance is a high probability for Andreev reflection at the NS boundary This is illustrated in fig 6, which shows the results of numerical simulations [39] of transport through a disordered normal region connected via a tunnel barrier to a superconductor The tunnel barrier is characterized by a transmission probability per mode Γ The dash dotted lines refer to an ideal interface ($\Gamma = 1$), and show the conductance *dip* due to weak localization, discussed above For $\Gamma \simeq 0\,2$– $0\,4$ the data for G_{NS} (filled circles) shows a crossover[*] to a conductance *peak* This is the phenomenon of *reflectionless tunneling*, discussed in the following section

[*] The crossover is accompanied by an overshoot around $eV \approx \Gamma_c$ indicating the absence of an excess current (i e the linear I–V characteristic for $eV \gg \Gamma_c$ extrapolates back through the origin) We do not have an analytical explanation for the overshoot
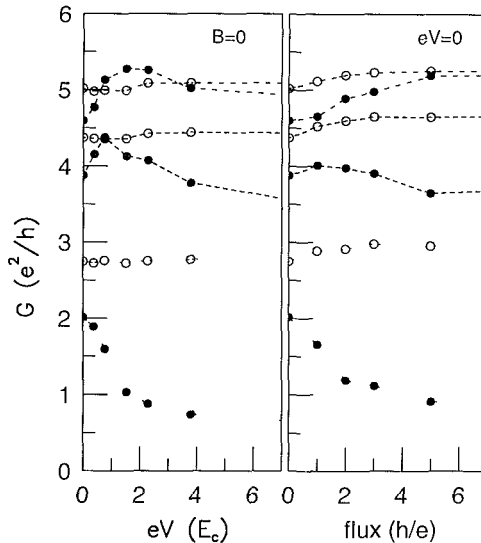
Fig 6   Voltage and magnetic field dependence of G_{NS} (filled circles) and G_N (open circles) Numerical simulation of a disordered normal region ($L/W = 4\,8$, $l/L = 0\,12$, $N = 14$) in series with a tunnel barrier (transmission probability per mode Γ, dotted lines $\Gamma = 0\,2$, dashed $\Gamma = 0\,6$, dash-dotted $\Gamma = 1$) Note the crossover from a *dip* (weak localization) to a *peak* (reflectionless tunneling) in G_{NS} on reducing Γ (From ref [39])

5. Reflectionless tunneling

In 1991, Kastalsky et al. [41] discovered a large and narrow peak in the differential conductance of a Nb–InGaAs junction. We reproduce their data in fig. 7. (A similar peak is observed as a function of magnetic field.) Since then a great deal of experimental [42–48], numerical [39,49], and analytical work [50–54] has been done on this effect. Here we focus on the explanation in terms of *disorder-induced opening of tunneling channels* [30,54], which is the most natural from the view point of the scattering formula (2 22), and which we feel captures the essence of the effect. Equivalently, the conductance peak can be explained in terms of a non-equilibrium proximity effect, which is the preferred explanation in a Green's function formulation of the problem [52,55–57]. We begin by reviewing the numerical work [39].

5.1. Numerical simulations

A sharp peak in the conductance around $V, B = 0$ is evident in the numerical simulations for $\Gamma = 0.2$ (dotted lines in fig. 6). While G_N depends only weakly on B
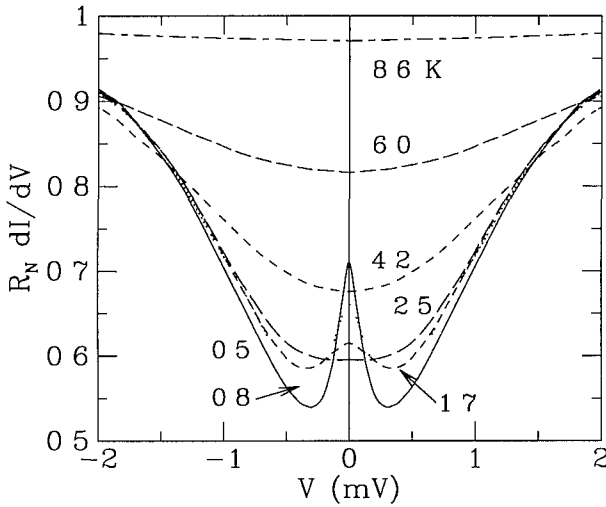
Fig 7   Differential conductance (normalized by the normal-state resistance $R_N = 0\,27\,\Omega$) as a function of applied voltage at seven different temperatures   Experimental data by Kastalsky et al for a Nb–InGaAs junction   Note the difference with fig 5   A peak rather than a dip develops at the lowest temperatures   and the size of the peak ($0\,6\,\Omega^{-1} \simeq 1\,5 \times 10^4\,e^2/h$) is four orders of magnitude greater   The width of the peak is comparable to the width of the dip in fig 5   (From ref [41])

and V in this range (open circles), G_{NS} drops abruptly (filled circles)   The width of the conductance peak in B and eV is respectively of order $B_c = h/eLW$ (one flux quantum through the normal region) and $eV_c = \pi\hbar D/L^2 \equiv E_c$ (the Thouless energy)   The width of the peak is the same as the width of the conductance dip due to weak localization, which occurs for larger barrier transparencies   The size of the peak is much greater than the dip, however

It is instructive to first discuss the *classical* resistance $R_{\mathrm{NS}}^{\mathrm{class}}$ of the NS junction   The basic approximation in $R_{\mathrm{NS}}^{\mathrm{class}}$ is that currents rather than amplitudes are matched at the NS interface [31]   The result is

$$R_{\mathrm{NS}}^{\mathrm{class}} = (h/2Ne^2)\left[L/l + 2\Gamma^{-2} + \mathcal{O}(1)\right] \tag{5 1}$$

The contribution from the barrier is $\propto \Gamma^{-2}$ because tunneling into a superconductor is a two-particle process [58]   Both the incident electron and the Andreev-reflected hole have to tunnel through the barrier (the net result being the addition of a Cooper pair to the superconducting condensate [1])   Equation (5 1) is to be contrasted with the classical resistance $R_{\mathrm{N}}^{\mathrm{class}}$ in the normal state,

$$R_{\mathrm{N}}^{\mathrm{class}} = (h/2Ne^2)\left[L/l + \Gamma^{-1} + \mathcal{O}(1)\right], \tag{5 2}$$

where the contribution of a resistive barrier is $\propto \Gamma^{-1}$ In the absence of a tunnel
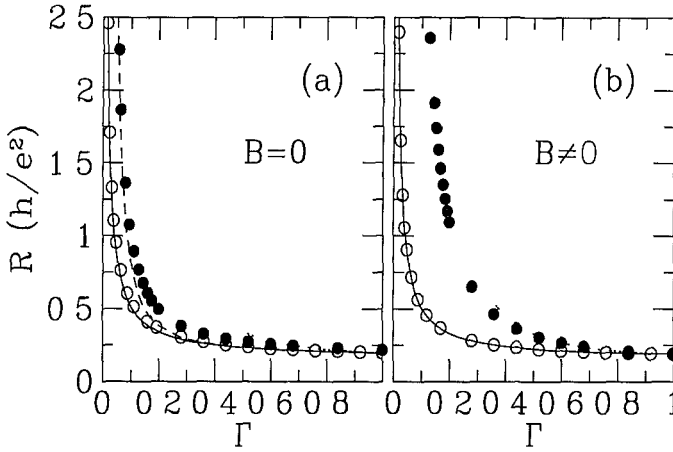
Fig 8 Filled circles Numerically calculated resistance R_{NS} of a disordered NS junction versus the transmission probability per mode Γ of the tunnel barrier at the NS interface Open circles Resistance R_N of the same junction in the normal state (a) is for zero magnetic field (b) is for a flux of $10\,h/e$ through the disordered region The dotted and solid curves are the classical eqs (5 1) and (5 2) The dashed curve is the theory of ref [52] which for $\Gamma \gg l/L \approx 0\,12$ coincides with eq (5 3) (From ref [39])

barrier (i e for $\Gamma = 1$), $R_{NS}^{\text{class}} = R_N^{\text{class}}$ for $L \gg l$, in agreement with refs [31,32] Let us now see how these classical results compare with the simulations [39]

In fig 8 we show the resistance (at $V = 0$) as a function of Γ in the absence and presence of a magnetic field (The parameters of the disordered region are the same as for fig 6) There is good agreement with the classical eqs (5 1) and (5 2) for a magnetic field corresponding to 10 flux quanta through the disordered segment (fig 8b) For $B = 0$, however, the situation is different (fig 8a) The normal-state resistance (open circles) still follows approximately the classical formula (solid curve) (Deviations due to weak localization are noticeable, but small on the scale of the figure) In contrast, the resistance of the NS junction (filled circles) lies much below the classical prediction (dotted curve) The numerical data shows that for $\Gamma \gg l/L$ one has approximately

$$R_{NS}(B = 0, V = 0) \approx R_N^{\text{class}}, \tag{5 3}$$

which for $\Gamma \ll 1$ is much smaller than R_{NS}^{class} This is the phenomenon of *reflectionless tunneling* In fig 8a the barrier contributes to R_{NS} in order Γ^{-1}, just as for single-particle tunneling, and not in order Γ^{-2}, as expected for two-particle tunneling It is as if the Andreev-reflected hole is not reflected by the barrier The interfering trajectories responsible for this effect were first identified by Van Wees

et al [50] The numerical data of fig 8a is in good agreement with the Green's function calculation of Volkov, Zaĭtsev, and Klapwijk [52] (dashed curve) Both these papers have played a crucial role in the understanding of the effect The scaling theory reviewed below [54] is essentially equivalent to the Green's function calculation, but has the advantage of explicitly demonstrating how the opening of tunneling channels on increasing the length L of the disordered region induces a transition from a Γ^{-2} dependence to a Γ^{-1} dependence when $L \simeq l/\Gamma$

5 2 Scaling theory

We use the parameterization

$$T_n = \frac{1}{\cosh^2 x_n}, \tag{5 4}$$

similar to eq (3 9), but now with a dimensionless variable $x_n \in [0, \infty)$ The density of the x-variables, for a length L of disordered region, is denoted by

$$\rho(x, L) = \langle \sum_n \delta(x - x_n) \rangle_L \tag{5 5}$$

For $L = 0$, i e in the absence of disorder, we have the initial condition imposed by the barrier,

$$\rho(x, 0) = N \delta(x - x_0), \tag{5 6}$$

with $\Gamma = 1/\cosh^2 x_0$ The scaling theory describes how $\rho(x, L)$ evolves with increasing L This evolution is governed by the equation

$$\frac{\partial}{\partial s} \rho(x, s) = -\frac{1}{2N} \frac{\partial}{\partial x} \rho(x, s) \frac{\partial}{\partial x} \int_0^\infty dx' \, \rho(x', s) \ln |\sinh^2 x - \sinh^2 x'|, \tag{5 7}$$

where we have defined $s \equiv L/l$ This non-linear diffusion equation was derived by Mello and Pichard [59] from a Fokker–Planck equation [34,60,61] for the joint distribution function of all N eigenvalues, by integrating out $N - 1$ eigenvalues and taking the large-N limit This limit restricts its validity to the metallic regime ($N \gg L/l$), and is sufficient to determine the leading order contribution to the average conductance, which is $\mathcal{O}(N)$ The weak-localization correction, which is $\mathcal{O}(1)$, is neglected here A priori, eq (5 7) holds only for a "quasi-one-dimensional" wire geometry (length L much greater than width W), because the Fokker–Planck equation from which it is derived requires $L \gg W$ Numerical simulations indicate that the geometry dependence only appears in the $\mathcal{O}(1)$ corrections, and that the $\mathcal{O}(N)$ contributions are essentially the same for a wire, square, or cube

In ref [54] it is shown how the scaling equation (5 7) can be solved exactly, for arbitrary initial condition $\rho(x, 0) \equiv \rho_0(x)$ The method of solution is based
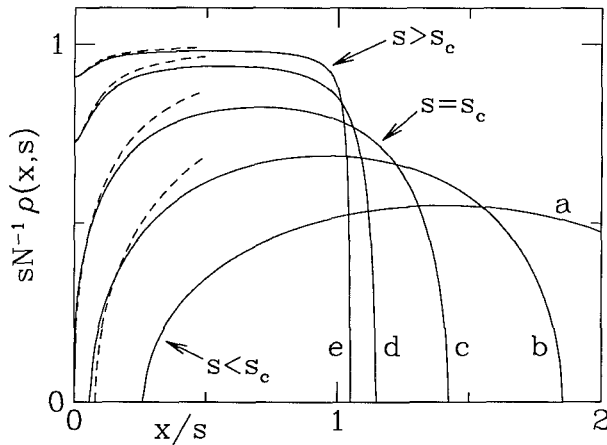
Fig 9 Eigenvalue density $\rho(x, s)$ as a function of x (in units of $s = L/l$) for $\Gamma = 0\,1$ Curves a,b,c,d,e are for $s = 2, 4, 9, 30, 100$, respectively The solid curves are from eq (5 8), the dashed curves from eq (5 12) The collision of the density profile with the boundary at $x = 0$, for $s = s_c = (1 - \Gamma)/\Gamma$, signals the disorder-induced opening of tunneling channels responsible for the reflectionless tunneling effect (From ref [54])

on a mapping of eq. (5 7) onto Euler's equation for the isobaric flow of a two-dimensional ideal fluid· L corresponds to time and ρ to the y-component of the velocity field on the x-axis. [Please note that in this section x is the auxiliary variable defined in eq. (5 4) and *not* the physical coordinate in fig. 2] The result is

$$\rho(x, s) = (2N/\pi)\,\mathrm{Im}\,U(x - \iota 0^+, s), \tag{5.8}$$

where the complex function $U(z, s)$ is determined by

$$U(z, s) = U_0\big(z - sU(z, s)\big). \tag{5 9}$$

The function $U_0(z)$ is fixed by the initial condition,

$$U_0(z) = \frac{\sinh 2z}{2N} \int_0^\infty dx' \, \frac{\rho_0(x')}{\sinh^2 z - \sinh^2 x'}. \tag{5.10}$$

The implicit equation (5.9) has multiple solutions in the entire complex plane; We need the solution for which both z and $z - sU(z, s)$ lie in the strip between the lines $y = 0$ and $y = -\pi/2$, where $z = x + iy$.

The initial condition (5.6) corresponds to

$$U_0(z) = \tfrac{1}{2} \sinh 2z \, (\cosh^2 z - \Gamma^{-1})^{-1} \tag{5 11}$$

The resulting density (5 8) is plotted in fig 9 (solid curves), for $\Gamma = 0\ 1$ and several values of s For $s \gg 1$ and $x \ll s$ it simplifies to

$$x = \tfrac{1}{2}\operatorname{arccosh} \tau - \tfrac{1}{2}\Gamma s(\tau^2 - 1)^{1/2} \cos \sigma,$$

$$\sigma \equiv \pi s N^{-1} \rho(x, s), \quad \tau \equiv \sigma(\Gamma s \sin \sigma)^{-1}, \tag{5 12}$$

shown dashed in fig 9 Equation (5 12) agrees with the result of a Green's function calculation by Nazarov [30] For $s = 0$ (no disorder), ρ is a delta function at x_0 On adding disorder the eigenvalue density rapidly spreads along the x-axis (curve a), such that $\rho \leq N/s$ for $s > 0$ The sharp edges of the density profile, so uncharacteristic for a diffusion profile, reveal the hydrodynamic nature of the scaling equation (5 7) The upper edge is at

$$x_{\max} = s + \tfrac{1}{2} \ln(s/\Gamma) + \mathcal{O}(1) \tag{5 13}$$

Since L/x has the physical significance of a localization length [34], this upper edge corresponds to a minimum localization length $\xi_{\min} = L/x_{\max}$ of order l The lower edge at $x_{\min}$ propagates from x_0 to 0 in a "time" $s_c = (1 - \Gamma)/\Gamma$ For $1 \ll s \leq s_c$ one has

$$x_{\min} = \tfrac{1}{2}\operatorname{arccosh}(s_c/s) - \tfrac{1}{2}[1 - (s/s_c)^2]^{1/2} \tag{5 14}$$

It follows that the maximum localization length $\xi_{\max} = L/x_{\min}$ *increases* if disorder is added to a tunnel junction This paradoxical result, that disorder enhances transmission, becomes intuitively obvious from the hydrodynamic correspondence, which implies that $\rho(x, s)$ spreads both to larger *and* smaller x as the fictitious time s progresses When $s = s_c$ the diffusion profile hits the boundary at $x = 0$ (curve c), so that $x_{\min} = 0$ This implies that for $s > s_c$ there exist scattering states (eigenfunctions of $tt^\dagger$) which tunnel through the barrier with near-unit transmission probability, even if $\Gamma \ll 1$ The number N_{open} of transmission eigenvalues close to one (*open channels*) is of the order of the number of x_n's in the range 0 to 1 (since $T_n \equiv 1/\cosh^2 x_n$ vanishes exponentially if $x_n > 1$) For $s \gg s_c$ (curve e) we estimate

$$N_{\text{open}} \simeq \rho(0, s) = N(s + \Gamma^{-1})^{-1}, \tag{5 15}$$

where we have used eq (5 12) The disorder induced opening of tunneling channels was discovered by Nazarov [30] It is the fundamental mechanism for the Γ^{-2} to Γ^{-1} transition in the conductance of an NS junction, as we now discuss

According to eqs (2 22), (2 23), (5 4), and (5 5), the average conductances $\langle G_{\text{NS}} \rangle$ and $\langle G_{\text{N}} \rangle$ are given by the integrals

$$\langle G_{\text{NS}} \rangle = \frac{4e^2}{h} \int_0^\infty dx\, \rho(x, s) \cosh^{-2} 2x, \tag{5 16}$$

$$\langle G_{\text{N}} \rangle = \frac{2e^2}{h} \int_0^\infty dx\, \rho(x, s) \cosh^{-2} x \tag{5 17}$$

Here we have used the same trigonometric identity as in eq (4 1) For $\Gamma \gg l/L$ one is in the regime $s \gg s_c$ of curve e in fig 9 Then the dominant contribution to the integrals comes from the range $x/s \ll 1$ where $\rho(x,s) \approx \rho(0,s) = N(s + \Gamma^{-1})^{-1}$ is approximately independent of x Substitution of $\rho(x,s)$ by $\rho(0,s)$ in eqs (5 16) and (5 17) yields directly

$$\langle G_{NS} \rangle \approx \langle G_N \rangle \approx 1/R_N^{class}, \tag{5 18}$$

in agreement with the result (5 3) of the numerical simulations

Equation (5 18) has the linear Γ dependence characteristic for reflectionless tunneling The crossover to the quadratic Γ dependence when $\Gamma \lesssim l/L$ is obtained by evaluating the integrals (5 16) and (5 17) with the density $\rho(x,s)$ given by eq (5 8) The result is [54]

$$\langle G_{NS} \rangle = (2Ne^2/h)(s + Q^{-1})^{-1}, \tag{5 19}$$

$$\langle G_N \rangle = (2Ne^2/h)(s + \Gamma^{-1})^{-1} \tag{5 20}$$

The "effective" tunnel probability Q is defined by

$$Q = \frac{\theta}{s \cos \theta} \left(\frac{\theta}{\Gamma s \cos \theta}(1 + \sin \theta) - 1 \right), \tag{5 21}$$

where $\theta \in (0, \pi/2)$ is the solution of the transcendental equation

$$\theta[1 - \tfrac{1}{2}\Gamma(1 - \sin \theta)] = \Gamma s \cos \theta \tag{5 22}$$

For $\Gamma \ll 1$ (or $s \gg 1$) eqs (5 21) and (5 22) simplify to $Q = \Gamma \sin \theta$, $\theta = \Gamma s \cos \theta$, in precise agreement with the Green's function calculation of Volkov, Zaïtsev, and Klapwijk [52] According to eq (5 20), the normal state resistance increases *linearly* with the length L of the disordered region, as expected from Ohm's law This classical reasoning fails if one of the contacts is in the superconducting state The scaling of the resistance $R_{NS} \equiv 1/\langle G_{NS} \rangle$ with length, computed from eq (5 19), is plotted in fig 10 For $\Gamma = 1$ the resistance increases monotonically with L The ballistic limit $L \to 0$ equals $h/4Ne^2$, half the contact resistance of a normal junction because of Andreev reflection (cf section 3 1) For $\Gamma \lesssim 0\,5$ a *resistance minimum* develops, somewhat below $L = l/\Gamma$ The resistance minimum is associated with the crossover from a quadratic to a linear dependence of R_{NS} on $1/\Gamma$

If $\Gamma s \gg 1$ one has $\theta \to \pi/2$, hence $Q \to \Gamma$ In the opposite regime $\Gamma s \ll 1$ one has $\theta \to \Gamma s$, hence $Q \to \Gamma^2 s$ The corresponding asymptotic expressions for $\langle G_{NS} \rangle$ are (assuming $\Gamma \ll 1$ and $s \gg 1$)

$$\langle G_{NS} \rangle = (2Ne^2/h)(s + \Gamma^{-1})^{-1}, \text{ if } \Gamma s \gg 1, \tag{5 23}$$

$$\langle G_{NS} \rangle = (2Ne^2/h)\Gamma^2 s, \text{ if } \Gamma s \ll 1 \tag{5 24}$$
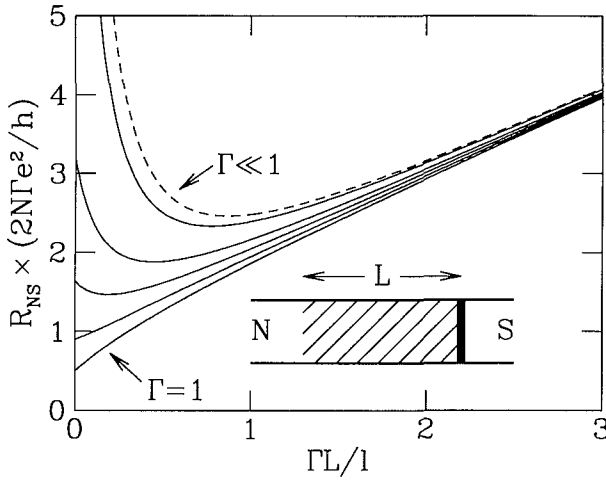
Fig 10 Dependence of the resistance R_{NS} on the length L of the disordered normal region (hatched in the inset), for different values of the transmittance Γ of the NS interface Solid curves are computed from eq (5 19), for $\Gamma = 1$ 0 8, 0 6, 0 4 0 1 from bottom to top For $\Gamma \ll 1$ the dashed curve is approached (From ref [54])

In either limit the conductance is greater than the classical result

$$G_{NS}^{class} = (2Ne^2/h)(s + 2\Gamma^{-2})^{-1}, \tag{5 25}$$

which holds if phase coherence between electrons and holes is destroyed by a voltage or magnetic field The peak in the conductance around $V, B = 0$ is of order $\Delta G_{NS} = \langle G_{NS} \rangle - G_{NS}^{class}$, which has the relative magnitude

$$\frac{\Delta G_{NS}}{\langle G_{NS} \rangle} \approx \frac{2}{2 + \Gamma^2 s} \tag{5 26}$$

The scaling theory assumes zero temperature Hekking and Nazarov [53] have studied the conductance of a resistive NS interface at finite temperatures, when L is greater than the correlation length $L_c = \min(l_\phi, \sqrt{\hbar D/k_B T})$ Their result is consistent with the limiting expression (5 24), if $s = L/l$ is replaced by L_c/l The implication is that, if $L > L_c$, the non-linear scaling of the resistance shown in fig 10 only applies to a disordered segment of length L_c adjacent to the superconductor For the total resistance one should add the Ohmic contribution of order $(h/e^2)(L - L_c)/l$ from the rest of the wire

5 3   Double-barrier junction

In the previous subsection we have discussed how the opening of tunneling channels (i e the appearance of transmission eigenvalues close to one) by disorder leads to a minimum in the resistance when $L \simeq l/\Gamma$ The minimum separates a Γ^{-1} from a Γ^{-2} dependence of the resistance on the transparency of the interface We referred to the Γ^{-1} dependence as "reflectionless tunneling", since it is as if one of the two quasiparticles which form the Cooper pair can tunnel through the barrier with probability one In the present subsection we will show, following ref [62], that a qualitatively similar effect occurs if the disorder in the normal region is replaced by a second tunnel barrier (tunnel probability Γ') The resistance at fixed Γ shows a minimum as a function of Γ' when $\Gamma' \simeq \Gamma$ For $\Gamma' \lesssim \Gamma$ the resistance has a Γ^{-1} dependence, so that we can speak again of reflectionless tunneling

We consider an NI_1NI_2S junction, where N = normal metal, S = superconductor, and I_i = insulator or tunnel barrier (transmission probability per mode $\Gamma_i \equiv 1/\cosh^2 \alpha_i$) We assume ballistic motion between the barriers (The effect of disorder is discussed later) A straightforward calculation yields the transmission probabilities T_n of the two barriers in series,

$$T_n = (a + b \cos \varphi_n)^{-1}, \tag{5 27}$$

$$a = \tfrac{1}{2} + \tfrac{1}{2} \cosh 2\alpha_1 \cosh 2\alpha_2, \quad b = \tfrac{1}{2} \sinh 2\alpha_1 \sinh 2\alpha_2, \tag{5 28}$$

where φ_n is the phase accumulated between the barriers by mode n Since the transmission matrix t is diagonal, the transmission probabilities T_n are identical to the eigenvalues of $tt^\dagger$ We assume that $L \gg \lambda_\Gamma$ (λ_Γ is the Fermi wavelength) and $N\Gamma_i \gg 1$, so that the conductance is not dominated by a single resonance In this case, the phases φ_n are distributed uniformly in the interval $(0, 2\pi)$ and we may replace the sum over the transmission eigenvalues in eqs (2 22) and (2 23) by integrals over φ $\sum_{n=1}^{N} f(\varphi_n) \to (N/2\pi) \int_0^{2\pi} d\varphi \, f(\varphi)$ The result is

$$G_{NS} = \frac{4Ne^2}{h} \frac{\cosh 2\alpha_1 \cosh 2\alpha_2}{\left(\cosh^2 2\alpha_1 + \cosh^2 2\alpha_2 - 1\right)^{3/2}}, \tag{5 29}$$

$$G_N = \frac{4Ne^2}{h} (\cosh 2\alpha_1 + \cosh 2\alpha_2)^{-1} \tag{5 30}$$

These expressions are symmetric in the indices 1 and 2 It does not matter which of the two barriers is closest to the superconductor In the same way we can compute the entire distribution of the transmission eigenvalues, $\rho(T) \equiv \sum_n \delta(T - T_n) \to (N/2\pi) \int_0^{2\pi} d\varphi \, \delta(T - T(\varphi))$ Substituting $T(\varphi) = (a + b \cos \varphi)^{-1}$ from eq (5 27), one finds

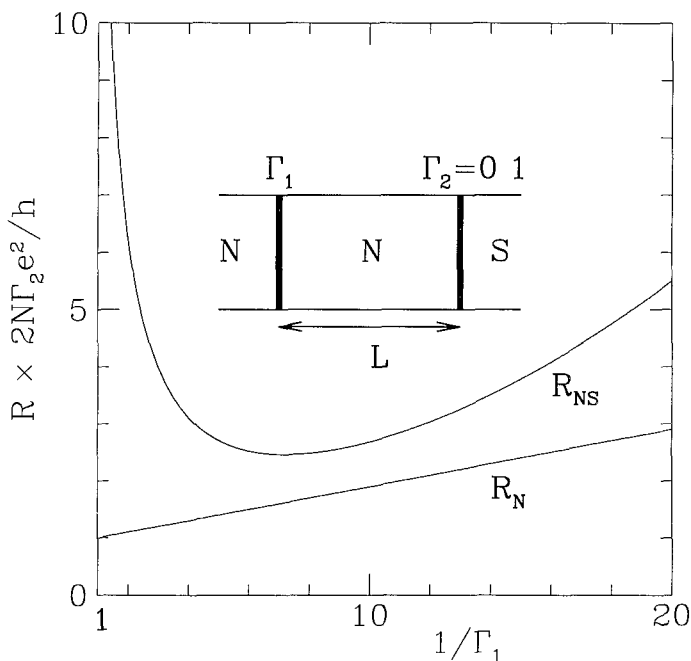$$\rho(T) = \frac{N}{\pi T} \left(b^2 T^2 - (aT - 1)^2\right)^{-1/2} \tag{5 31}$$

Fig 11   Dependence of the resistances R_N and R_{NS} of ballistic NININ and NINIS structures, respectively, on barrier transparency Γ_1, while transparency $\Gamma_2 = 0$ 1 is kept fixed [computed from eqs (5 29) and (5 30)] The inset shows the NINIS structure considered (From ref [62])

In fig 11 we plot the resistance $R_N = 1/G_N$ and $R_{NS} = 1/G_{NS}$, following from eqs (5 29) and (5 30) Notice that R_N follows Ohm's law,

$$R_N = \frac{h}{2Ne^2}(1/\Gamma_1 + 1/\Gamma_2 - 1), \qquad (5\ 32)$$

as expected from classical considerations In contrast, the resistance R_{NS} has a *minimum* if one of the Γ's is varied while keeping the other fixed This resistance minimum cannot be explained by classical series addition of barrier resistances If $\Gamma_2 \ll 1$ is fixed and Γ_1 is varied, as in fig 11, the minimum occurs when $\Gamma_1 = \sqrt{2}\Gamma_2$ The minimal resistance R_{NS}^{min} is of the same order of magnitude as the resistance R_N in the normal state at the same value of Γ_1 and Γ_2 In particular, we find that R_{NS}^{min} depends linearly on $1/\Gamma_1$, whereas for a single barrier $R_{NS} \propto 1/\Gamma^2$

The linear dependence on the barrier transparency shows the qualitative similarity of a ballistic NINIS junction to the disordered NIS junction considered in the previous subsection To illustrate the similarity, we compare in fig 12 the densit-
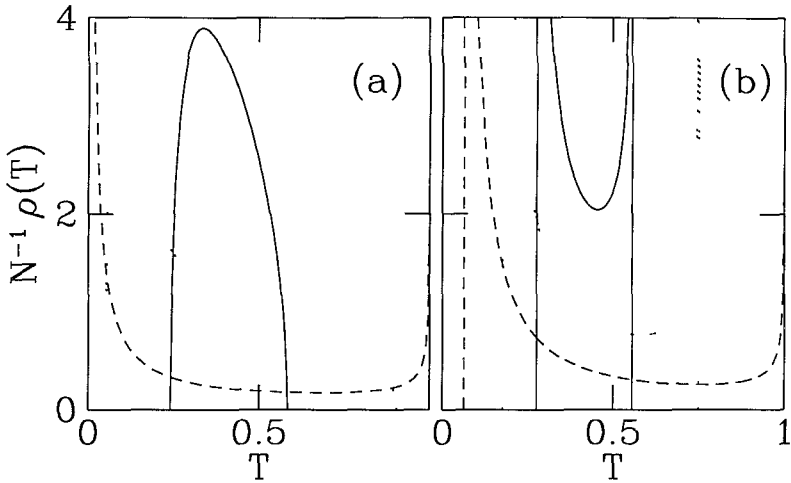
Fig 12 Density of transmission eigenvalues through a normal region containing a potential barrier (transmission probability $\Gamma = 0\ 4$) The left panel (a) shows the disorder induced opening of tunnel ing channels (solid curve $s = 0\ 04$ dotted $s = 0\ 4$, dashed $s = 5$ where $s \equiv L/l$) The right panel (b) shows the opening of channels by a second tunnel barrier (transparency Γ', solid curve $\Gamma' = 0\ 95$, dotted $\Gamma' = 0\ 8$, dashed $\Gamma' = 0\ 4$) The curves in (a) are computed from eq (5 8) the curves in (b) from eq (5 31) (From ref [62])

ies of normal-state transmission eigenvalues The left panel is for an NIS junction [computed using eq (5 8)], the right panel is for an NINIS junction [computed from eq (5 31)] In the NIS junction, disorder leads to a bimodal distribution $\rho(T)$, with a peak near zero transmission and another peak near unit transmission (dashed curve) A similar bimodal distribution appears in the ballistic NINIS junction, for approximately equal transmission probabilities of the two barriers There are also differences between the two cases The NIS junction has a unimodal $\rho(T)$ if $L/l < 1/\Gamma$, while the NINIS junction has a bimodal $\rho(T)$ for any ratio of Γ_1 and Γ_2 In both cases, the opening of tunneling channels, i e the appearance of a peak in $\rho(T)$ near $T = 1$, is the origin for the $1/\Gamma$ dependence of the resistance

The scaling equation of section 5 2 can be used to investigate what happens to the resistance minimum if the region of length L between the tunnel barriers contains impurities, with elastic mean free path l As shown in ref [62], the resistance minimum persists as long as $l \gtrsim \Gamma L$ In the diffusive regime ($l \ll L$) the scaling theory is found to agree with the Green's function calculation by Volkov, Zaïtsev, and Klapwijk for a disordered NINIS junction [52] For strong barriers

$(\Gamma_1, \Gamma_2 \ll 1)$ and strong disorder $(L \gg l)$, one has the two asymptotic formulas

$$G_{\mathrm{NS}} = \frac{2Ne^2}{h} \frac{\Gamma_1^2 \Gamma_2^2}{(\Gamma_1^2 + \Gamma_2^2)^{3/2}}, \quad \text{if } \Gamma_1, \Gamma_2 \ll l/L, \tag{5 33}$$

$$G_{\mathrm{NS}} = \frac{2Ne^2}{h} (L/l + 1/\Gamma_1 + 1/\Gamma_2)^{-1}, \quad \text{if } \Gamma_1, \Gamma_2 \gg l/L \tag{5 34}$$

Equation (5 33) coincides with eq (5 29) in the limit $\alpha_1, \alpha_2 \gg 1$ (recall that $\Gamma_i \equiv 1/\cosh^2 \alpha_i$) This shows that the effect of disorder on the resistance minimum can be neglected as long as the resistance of the junction is dominated by the barriers In this case G_{NS} depends linearly on Γ_1 and Γ_2 only if $\Gamma_1 \approx \Gamma_2$ Equation (5 34) shows that if the disorder dominates, G_{NS} has a linear Γ-dependence regardless of the relative magnitude of Γ_1 and Γ_2

We have assumed zero temperature, zero magnetic field, and infinitesimal applied voltage Each of these quantities is capable of destroying the phase coherence between the electrons and the Andreev-reflected holes, which is responsible for the resistance minimum As far as the temperature T and voltage V are concerned, we require $k_{\mathrm{B}}T, eV \ll \hbar/\tau_{\mathrm{dwell}}$ for the appearance of a resistance minimum, where τ_{dwell} is the dwell time of an electron in the region between the two barriers For a ballistic NINIS junction $\tau_{\mathrm{dwell}} \simeq L/v_{\mathrm{F}}\Gamma$, while for a disordered junction $\tau_{\mathrm{dwell}} \simeq L^2/v_{\mathrm{F}}\Gamma l$ is larger by a factor L/l It follows that the condition on temperature and voltage becomes more restrictive if the disorder increases, even if the resistance remains dominated by the barriers As far as the magnetic field B is concerned, we require $B \ll h/eS$ (with S the area of the junction perpendicular to B), if the motion between the barriers is diffusive For ballistic motion the trajectories enclose no flux, so no magnetic field dependence is expected

A possible experiment to verify these results might be scanning tunneling microscopy (STM) of a metal particle on a superconducting substrate [63] The metal–superconductor interface has a fixed tunnel probability Γ_2 The probability Γ_1 for an electron to tunnel from STM to particle can be controlled by varying the distance (Volkov has recently analyzed this geometry in the regime that the motion from STM to particle is diffusive rather than by tunneling [64]) Another possibility is to create an NINIS junction using a two-dimensional electron gas in contact with a superconductor An adjustable tunnel barrier could then be implemented by means of a gate electrode

5 4 Circuit theory

The scaling theory of ref [54], which was the subject of section 5 2, describes the transition from the ballistic to the diffusive regime In the diffusive regime it is equivalent to the Green's function theory of ref [52] A third, equivalent,

theory for the diffusive regime was presented recently by Nazarov [65] Starting from a continuity equation for the Keldysh Green's function [66], and applying the appropriate boundary conditions [67], Nazarov was able to formulate a set of rules which reduce the problem of computing the resistance of an NS junction to a simple exercise in circuit theory Furthermore, the approach can be applied without further complications to multi-terminal networks involving several normal and superconducting reservoirs Because of its practical importance, we discuss Nazarov's circuit theory in some detail

The superconductors S_i should all be at the same voltage, but may have a different phase ϕ_i of the pair potential Zero temperature is assumed, as well as infinitesimal voltage differences between the normal reservoirs (linear response) The reservoirs are connected by a set of diffusive normal-state conductors (length L_i, mean free path l_i, $s_i \equiv L_i/l_i \gg 1$) Between the conductors there may be tunnel barriers (tunnel probability Γ_i) The presence of superconducting reservoirs has no effect on the resistance $(h/2Ne^2)s_i$ of the diffusive conductors, but affects only the resistance $h/2Ne^2\Gamma_i^{\mathrm{eff}}$ of the tunnel barriers The tunnel probability Γ_i of barrier i is renormalized to an effective tunnel probability Γ_i^{eff}, which depends on the entire circuit

Nazarov's rules to compute the effective tunnel probabilities are as follows To each node and to each terminal of the circuit one assigns a vector n_i of unit length For a normal reservoir, $n_i = (0, 0, 1)$ is at the north pole, for a superconducting reservoir, $n_i = (\cos\phi_i, \sin\phi_i, 0)$ is at the equator For a node, n_i is somewhere on the northern hemisphere The vector n_i is called a "spectral vector", because it is a particular parameterization of the local energy spectrum If the tunnel barrier is located between spectral vectors n_1 and n_2, its effective tunnel probability is[*]

$$\Gamma^{\mathrm{eff}} = (n_1 \quad n_2)\Gamma = \Gamma\cos\theta_{12}, \tag{5 35}$$

where θ_{12} is the angle between n_1 and n_2 The rule to compute the spectral vector of node i follows from the continuity equation for the Green's function Let the index k label the nodes or terminals connected to node i by a single tunnel barrier (with tunnel probability Γ_k) Let the index q label the nodes or terminals connected to i by a diffusive conductor (with $L/l \equiv s_q$) The spectral vectors then satisfy the sum rule [65]

$$\sum_k (n_i \times n_k)\Gamma_k + \sum_q (n_i \times n_q)\frac{\arccos(n_i \quad n_q)}{s_q\sqrt{1 - (n_i \quad n_q)^2}} = 0 \tag{5 36}$$

This is a sum rule for a set of vectors perpendicular to n_i of magnitude $\Gamma_k \sin\theta_{ik}$ or θ_{iq}/s_q, depending on whether the element connected to node i is a tunnel

---

[*] It may happen that $\cos\theta_{12} < 0$, in which case the effective tunnel probability is negative Nazarov has given an example of a four-terminal circuit with $\Gamma^{\mathrm{eff}} < 0$, so that the current through this barrier flows in the direction opposite to the voltage drop [68]
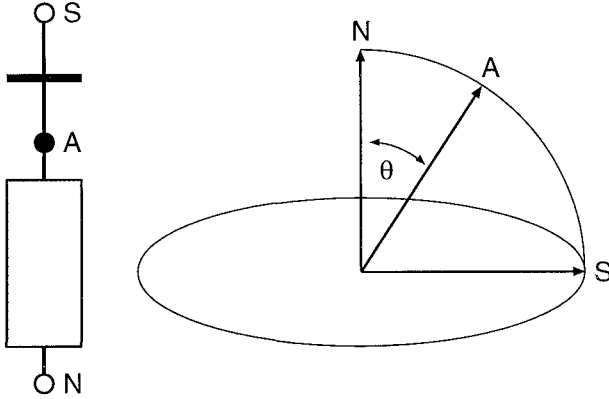
Fig. 13. At left: Circuit containing two terminals (open circles), one node (filled circle), and two elements: A diffusive conductor (shaded) and a tunnel barrier (black). At right: Spectral vectors associated with the terminals N,S and with the node A.

barrier or a diffusive conductor. There is a sum rule for each node, and together the sum rules determine the spectral vectors of the nodes.

As a simple example, let us consider the system of section 5.2, consisting of one normal terminal (N), one superconducting terminal (S), one node (labeled A), and two elements: A diffusive conductor (with $L/l \equiv s$) between N and A, and a tunnel barrier (tunnel probability Γ) between A and S (see fig. 13). There are three spectral vectors, n_N, n_S, and n_A. All spectral vectors lie in one plane. (This holds for any network with a single superconducting terminal.) The resistance of the circuit is given by $R = (h/2Ne^2)(s + 1/\Gamma^{\text{eff}})$, with the effective tunnel probability

$$\Gamma^{\text{eff}} = \Gamma \cos \theta_{AS} = \Gamma \sin \theta. \tag{5.37}$$

Here $\theta \in [0, \pi/2]$ is the polar angle of n_A. This angle is determined by the sum rule (5.36), which in this case takes the form

$$\Gamma \cos \theta - \theta/s = 0. \tag{5.38}$$

Comparison with section 5.2 shows that Γ^{eff} coincides with the effective tunnel probability Q of eq. (5.21) in the limit $s \gg 1$, i.e. if one restricts oneself to the diffusive regime. That is the basic requirement for the application of the circuit theory.

Let us now consider the "fork junction" of fig. 14, with one normal terminal (N) and two superconducting terminals S_1 and S_2 (phases $\phi_1 \equiv -\phi/2$ and $\phi_2 \equiv \phi/2$). There is one node (A), which is connected to N by a diffusive conductor ($L/l \equiv s$), and to S_1 and S_2 by tunnel barriers (Γ_1 and Γ_2). This structure was studied
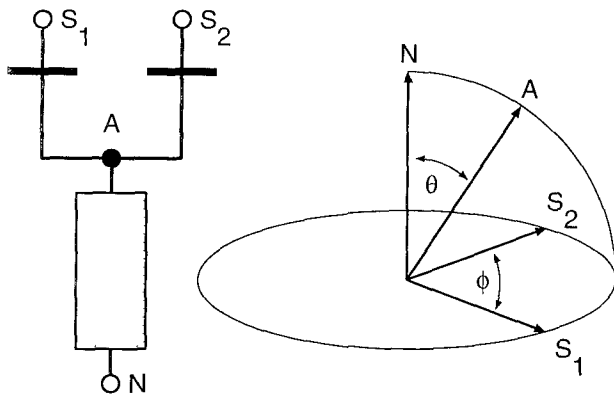
Fig 14. Circuit diagram and spectral vectors for a structure containing one normal and two superconducting terminals (phase difference ϕ).

theoretically by Hekking and Nazarov [53] and experimentally by Pothier et al. [69]. For simplicity, let us assume two identical tunnel barriers $\Gamma_1 = \Gamma_2 \equiv \Gamma$. Then the spectral vector $n_A = (\sin\theta, 0, \cos\theta)$ of node A lies symmetrically between the spectral vectors of terminals S_1 and S_2. The sum rule (5.36) now takes the form

$$2\Gamma |\cos\tfrac{1}{2}\phi| \cos\theta - \theta/s = 0. \tag{5.39}$$

Its solution determines the effective tunnel rate $\Gamma^{\text{eff}} = \Gamma|\cos\tfrac{1}{2}\phi| \sin\theta$ of each of the two barriers in parallel, and hence the conductance of the fork junction,

$$G = \frac{2Ne^2}{h}[s + \tfrac{1}{2}(\Gamma|\cos\tfrac{1}{2}\phi|\sin\theta)^{-1}]^{-1}. \tag{5.40}$$

Two limiting cases of eqs. (5.39) and (5.40) are

$$G = (2Ne^2/h)(s + \tfrac{1}{2}\Gamma^{-1}|\cos\tfrac{1}{2}\phi|^{-1})^{-1}, \quad \text{if } s\Gamma|\cos\tfrac{1}{2}\phi| \gg 1, \tag{5.41}$$

$$G = (4Ne^2/h)s\Gamma^2(1 + \cos\phi), \quad \text{if } s\Gamma|\cos\tfrac{1}{2}\phi| \ll 1. \tag{5.42}$$

For $\phi = 0$ (and $2\Gamma \to \Gamma$) these expressions reduce to the results (5.23) and (5.24) for an NS junction with a single superconducting reservoir. The limit (5.42) agrees with the finite-temperature result of Hekking and Nazarov [53], if s is replaced by L_c/l and a series resistance is added due to the normal segment which is further than a correlation length from the NS interfaces. The possibility of a dependence of the conductance on the superconducting phase difference was noted also in other theoretical works, for different geometries [70–75].

   The ϕ-dependence of the conductance of a fork junction has recently been observed by Pothier et al. [69]. Some of their data is reproduced in fig. 15. The
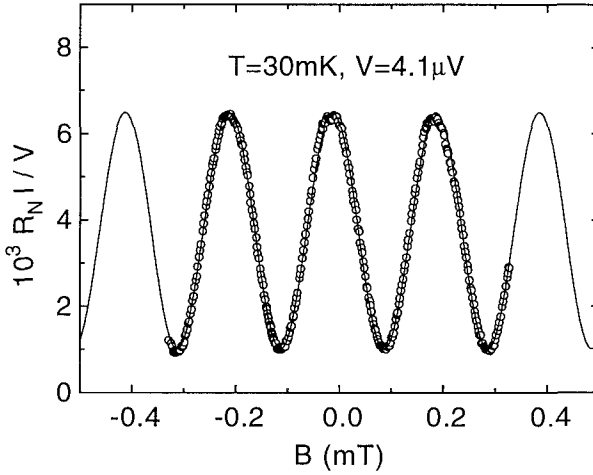
Fig 15 Conductance of a fork junction as a function of magnetic field, showing the dependence on the phase difference ϕ of the superconductor at two tunnel barriers The circles are measurements by Pothier et al [69] of the current I through a Cu wire connected to an oxidized Al fork (normal-state resistance $R_N = 1\,56\,\text{k}\Omega$) The applied voltage V is sufficiently low that I/V is close to the linear-response conductance (The amplitude of the oscillations at $V = 0$ is $3\,94 \times 10^{-6}\,\Omega^{-1}$, somewhat larger than in the figure) The solid curve is a cosine fit to the data The offset of maximum conductance from $B = 0$ is attributed to a small residual field in the cryostat (Courtesy of H Pothier)

conductance of a Cu wire attached to an oxidized Al fork oscillates as a function of the applied magnetic field. The period corresponds to a flux increment of $h/2e$ through the area enclosed by the fork and the wire, and thus to $\Delta\phi = 2\pi$. The experiment is in the regime where the junction resistance is dominated by the tunnel barriers, as in eq. (5.42).* The metal-oxide tunnel barriers in such structures have typically very small transmission probabilities ($\Gamma \simeq 10^{-5}$ in ref. [69]), so that the regime of eq (5.41) is not easily accessible. Larger Γ's can be realized by the Schottky barrier at a semiconductor — superconductor interface It would be of interest to observe the crossover with increasing Γ to the non-sinusoidal ϕ-dependence predicted by eq. (5.41), as a further test of the theory.

---

* Equation (5 42) provides only a qualitative description of the experiment, mainly because the motion in the arms of the fork is diffusive rather than ballistic This is why the conductance minima in fig 15 do not go to zero A solution of the diffusion equation in the actual experimental geometry is required for a quantitative comparison with the theory [69]

6. Universal conductance fluctuations

So far we have considered the *average* of the conductance over an ensemble of impurity potentials In fig 16 we show results of numerical simulations [39] for the *variance* of the sample-to-sample fluctuations of the conductance, as a function of the average conductance in the normal state A range of parameters L, W, l, N was used to collect this data, in the quasi-one-dimensional, metallic, diffusive regime $l < W < L < Nl$ An ideal NS interface was assumed ($\Gamma = 1$) The results for $\text{Var}\, G_N$ are as expected theoretically [34,35] for "universal conductance fluctuations" (UCF)

$$\text{Var}\, G_N = \frac{8}{15}\, \beta^{-1}(e^2/h)^2 \tag{6 1}$$

The index β equals 1 in the presence and 2 in the absence of time-reversal symmetry The $1/\beta$ dependence of $\text{Var}\, G_N$ implies that the variance of the conductance fluctuations is reduced by a factor of two upon application of a magnetic field, as observed in the simulation (see the two dotted lines in the lower part of fig 16) The data for $\text{Var}\, G_{NS}$ at $B = 0$ shows approximately a four-fold increase over $\text{Var}\, G_N$ For $B \neq 0$, the simulation shows that $\text{Var}\, G_{NS}$ is essentially *unaffected* by a time-reversal-symmetry breaking magnetic field In contrast to the situation in the normal state, the theory for UCF in an NS junction is quite different for zero and for non-zero magnetic field, as we now discuss

In zero magnetic field, the conductance of the NS junction is given by eq (2 22), which is an expression of the form $A = \sum_n a(T_n)$ Such a quantity A is called a *linear statistic* on the transmission eigenvalues The word "linear" refers to the fact that A does not contain products of different T_n's The function $a(T)$ may well depend non-linearly on T, as it does for G_{NS}, where $a(T)$ is a rational function of T The Landauer formula (2 23) for the normal-state conductance is also a linear statistic, with $a(\Gamma) \propto T$ It is a general theorem in random-matrix theory [76] that the variance of a linear statistic has a $1/\beta$ dependence on the symmetry index β Moreover, the magnitude of the variance is independent of the microscopic properties of the system (sample size, degree of disorder) This is Imry's fundamental explanation for UCF [28]

For a wire geometry, there exists a formula for the variance of an arbitrary linear statistic [37,77,78],

$$\text{Var}\, A = -\frac{1}{2\beta\pi^2} \int_0^1 dT \int_0^1 dT' \left(\frac{da(T)}{dT}\right)\left(\frac{da(T')}{dT'}\right)$$
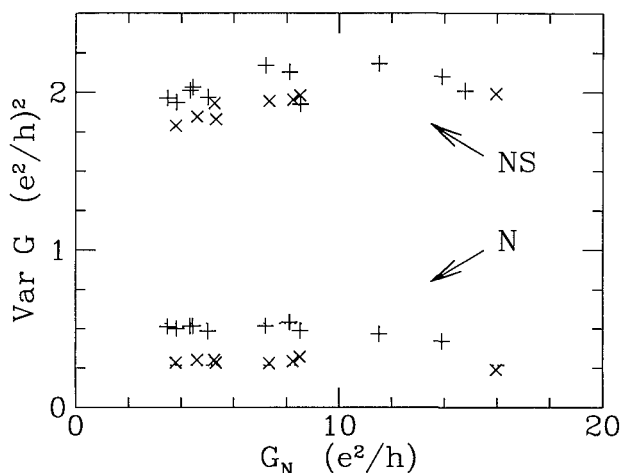$$\times \ln\left(\frac{1 + \pi^2[x(T) + x(T')]^{-2}}{1 + \pi^2[x(T) - x(T')]^{-2}}\right), \tag{6 2}$$

Fig 16 Numerical calculation of the variance of the fluctuations in G_N and G_{NS}, as a function of the average G_N (+ for $B = 0$, × for a flux of $10\,h/e$) Dotted lines are the analytical results from eqs (6 1) and (6 3) Note the absence of a factor of two reduction in Var G_{NS} on applying a magnetic field (From ref [39])

where $x(T) = \mathrm{arccosh}\,T^{-1/2}$ In the normal state, substitution of $a(T) = (2e^2/h)T$ into eq (6 2) reproduces the result (6 1) In the NS junction, substitution of $a(T) = (4e^2/h)T^2(2 - T)^{-2}$ yields, for the case $\beta = 1$ of zero magnetic field,

$$\mathrm{Var}\,G_{NS} = \frac{32}{15}(2 - 90\pi^{-4})(e^2/h)^2 = 4\,30\,\mathrm{Var}\,G_N \qquad (6\ 3)$$

A factor of four between Var G_{NS} and Var G_N was estimated by Takane and Ebisawa [33], by an argument similar to that which we described in section 4 for the weak-localization correction (A diagrammatic calculation by the same authors [79] gave a factor of six, presumably because only the dominant diagram was included) The numerical data in fig 16 is within 10 % of the theoretical prediction (6 3) (upper dotted line) Similar numerical results for Var G_{NS} in zero magnetic field were obtained in refs [33,80]

We conclude that UCF in zero magnetic field is basically the same phenomenon for G_N and G_{NS}, because both quantities are linear statistics for $\beta = 1$ If time-reversal symmetry (TRS) is broken by a magnetic field, the situation is qualitatively different For G_N, broken TRS does not affect the universality of the fluctuations, but merely reduces the variance by a factor of two No such simple behavior is to be expected for G_{NS}, since it is no longer a linear statistic for $\beta = 2$ That is a crucial distinction between eq (2 20) for G_{NS} and the Land-

auer formula (2 23) for G_N, which remains a linear statistic regardless of whether TRS is broken or not This expectation [15] of an anomalous β dependence of Var G_{NS} was borne out by numerical simulations [39], which showed that the conductance fluctuations in an NS junction without TRS remain independent of disorder, and of approximately the same magnitude as in the presence of TRS (compare $+$ and $\times$ data points in the upper part of fig 16) An analytical theory remains to be developed

7. Shot noise

The conductance, which we studied in the previous sections, is the *time-averaged* current I divided by the applied voltage V Time-dependent fluctuations $\delta I(t)$ in the current give additional information on the transport processes The zero-frequency noise power P is defined by

$$P = 4 \int_0^\infty dt \, \langle \delta I(t) \delta I(0) \rangle \tag{7 1}$$

At zero temperature, the discreteness of the electron charge is the only source of fluctuations in time of the current These fluctuations are known as "shot noise", to distinguish them from the thermal noise at non-zero temperature A further distinction between the two is that the shot-noise power is proportional to the applied voltage, whereas the thermal noise does not vanish at $V = 0$ Shot noise is therefore an intrinsically non-equilibrium phenomenon If the transmission of an elementary charge e can be regarded as a sequence of uncorrelated events, then $P = 2e|I| \equiv P_{\text{Poisson}}$ as in a Poisson process In this section we discuss, following ref [81], the enhancement of shot noise in an NS junction The enhancement originates from the fact that the current in the superconductor is carried by Cooper pairs in units of $2e$ However, as we will see, a simple factor-of-two enhancement applies only in certain limiting cases

In the normal state, the shot-noise power (at zero temperature and infinitesimal applied voltage) is given by [82]

$$P_N = P_0 \text{Tr} \, tt^\dagger (1 - tt^\dagger) = P_0 \sum_{n=1}^N T_n (1 - T_n), \tag{7 2}$$

with $P_0 \equiv 2e|V|(2e^2/h)$ Equation (7 2) is the multi-channel generalization of earlier single-channel formulas [83,84] It is a consequence of the Pauli principle that closed ($T_n = 0$) as well as open ($T_n = 1$) scattering channels do not fluctuate and therefore give no contribution to the shot noise In the case of a tunnel barrier, all transmission eigenvalues are small ($T_n \ll 1$, for all n), so that the quadratic terms in eq (7 2) can be neglected Then it follows from comparison with eq

(2 23) that $P_\mathrm{N} = 2e|V|G_\mathrm{N} = 2e|I| = P_\mathrm{Poisson}$ In contrast, for a quantum point contact $P_\mathrm{N} \ll P_\mathrm{Poisson}$ Since on the plateaus of quantized conductance all the T_n's are either 0 or 1, the shot noise is expected to be only observable at the steps between the plateaus [84] For a diffusive conductor of length L much longer than the elastic mean free path l, the shot noise $P_\mathrm{N} = \frac{1}{3}P_\mathrm{Poisson}$ is one-third the Poisson noise, as a consequence of noiseless open scattering channels [85,86]

The analogue of eq (7 2) for the shot-noise power of an NS junction is [81]

$$P_\mathrm{NS} = 4P_0 \mathrm{Tr}\, s_\mathrm{he}s_\mathrm{he}^\dagger (1 - s_\mathrm{he}s_\mathrm{he}^\dagger) = P_0 \sum_{n=1}^{N} \frac{16T_n^2(1 - T_n)}{(2 - T_n)^4}, \tag{7 3}$$

where we have used eq (2 17) (with $\varepsilon = 0$) to relate the scattering matrix s_he for Andreev reflection to the transmission eigenvalues T_n of the normal region This requires zero magnetic field As in the normal state, scattering channels which have $T_n = 0$ or $T_n = 1$ do not contribute to the shot noise However, the way in which partially transmitting channels contribute is entirely different from the normal state result (7 2)

Consider first an NS junction without disorder, but with an arbitrary transmission probability Γ per mode of the interface In the normal state, eq (7 2) yields $P_\mathrm{N} = (1 - \Gamma)P_\mathrm{Poisson}$, implying full Poisson noise for a high tunnel barrier ($\Gamma \ll 1$) For the NS junction we find from eq (7 3)

$$P_\mathrm{NS} = P_0 N \frac{16\Gamma^2(1 - \Gamma)}{(2 - \Gamma)^4} = \frac{8(1 - \Gamma)}{(2 - \Gamma)^2} P_\mathrm{Poisson}, \tag{7 4}$$

where in the second equality we have used eq (2 22) This agrees with results obtained by Khlus [83], and by Muzykantskiĭ and Khmel'nitskiĭ [87], using different methods If $\Gamma < 2(\sqrt{2} - 1) \approx 0\ 83$, one observes a shot noise above the Poisson noise For $\Gamma \ll 1$ one has

$$P_\mathrm{NS} = 4e|I| = 2P_\mathrm{Poisson}, \tag{7 5}$$

which is a doubling of the shot-noise power divided by the current with respect to the normal-state result This can be interpreted as uncorrelated current pulses of $2e$-charged particles

Consider next an NS junction with a disordered normal region, but with an ideal interface ($\Gamma = 1$) We may then apply the formula (3 10) for the average of a linear statistic on the transmission eigenvalues to eqs (2 22) and (7 3) The result is

$$\frac{\langle P_\mathrm{NS} \rangle}{\langle G_\mathrm{NS} \rangle} = \frac{2}{3} \frac{P_0}{2e^2/h} \;\Rightarrow\; \langle P_\mathrm{NS} \rangle = \frac{4}{3}e|I| = \frac{2}{3}P_\mathrm{Poisson} \tag{7 6}$$

Equation (7 6) is twice the result in the normal state, but still smaller than the Poisson noise Corrections to (7 6) are of lower order in N and due to quantum-interference effects [88]
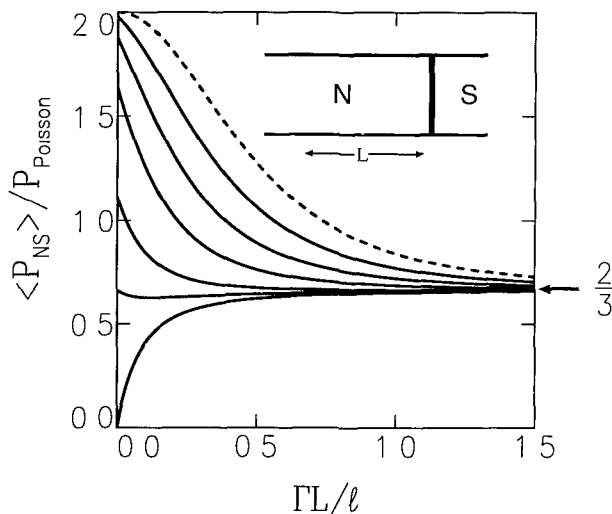
Fig 17 The shot noise power of an NS junction (in units of $P_{\text{Poisson}} \equiv 2e|I|$) as a function of the length L (in units of l/Γ) for barrier transparencies $\Gamma = 1\ 0\ 9\ 0\ 8\ 0\ 6\ 0\ 4\ 0\ 2$ from bottom to top The dashed curve gives the limiting result for $\Gamma \ll 1$ For $L = 0$ the noise power varies as a function of Γ according to eq (7 4) between doubled shot noise ($\langle P_{\text{NS}} \rangle = 4e|I|$) for a high barrier ($\Gamma \ll 1$) and zero in the absence of a barrier ($\Gamma = 1$) For $L \to \infty$ the noise power approaches the limiting value $\langle P_{\text{NS}} \rangle = \frac{4}{3}e|I|$ for each Γ (From ref [81])

Finally, consider an NS junction which contains a disordered normal region (length L, mean free path l) as well as a non ideal interface The scaling theory of section 5 2 has been applied to this problem in ref [81] Results are shown in fig 17, where $\langle P_{\text{NS}} \rangle / P_{\text{Poisson}}$ is plotted against $\Gamma L / l$ for various Γ Note the crossover from the ballistic result (7 4) to the diffusive result (7 6) For a high barrier ($\Gamma \ll 1$), the shot noise decreases from twice the Poisson noise to two-thirds the Poisson noise as the amount of disorder increases

8. Conclusion

We have reviewed a scattering approach to phase coherent transport accross the interface between a normal metal and a superconductor For the reflectionless tunneling phenomenon, the complete equivalence has been demonstrated to the non-equilibrium Green's function approach (The other effects we discussed have so far mainly been treated in the scattering approach) Although mathematically

equivalent, the physical picture offered by the two approaches is quite different
We chose to focus on the scattering approach because it makes direct contact with
the quantum interference effects studied extensively in the normal state The same
techniques used for weak localization and universal conductance fluctuations in
normal conductors could be used to study the modifications by Andreev reflection
in an NS junction

In the limit of zero voltage, zero temperature, and zero magnetic field, the
transport properties of the NS junction are determined entirely by the transmis-
sion eigenvalues T_n of the normal region A scaling theory for the distribution
of the T_n's then allows one to obtain analytical results for the mean and vari
ance of any observable of the form $A = \sum_n a(T_n)$ The conductance is of this
form, as well as the shot-noise power The only difference with the normal state
is the functional form of $a(T)$ (polynomial in the normal state, rational function
for an NS junction), so that the general results of the scaling theory [valid for
any function $a(T)$] can be applied at once At finite V, T, or B, one needs the
entire scattering matrix of the normal region, not just the transmission eigenval-
ues This poses no difficulty for a numerical calculation, as we have shown in
several examples However, analytical progress using the scattering approach
becomes cumbersome, and a diagrammatic Green's function calculation is more
efficient

Note added February 1995

The theory of section 4 has been extended to non-zero voltage and magnetic field
by P W Brouwer and the author (Phys Rev B **52** (1995) R3868) The results are
$\delta G_{\mathrm{NS}}(V = 0, B \neq 0) = \frac{1}{3}e^2/h$, $\delta G_{\mathrm{NS}}(V \neq 0, B = 0) = \frac{2}{3}e^2/h$, $\delta G_{\mathrm{NS}}(V \neq 0, B \neq 0) = 0$ The disagreement with the numerical simulations discussed in
section 4 is due to an insufficiently large system size

References

[1] A F Andreev, Zh Eksp Teor Fiz **46** (1964) 1823 [Sov Phys JETP **19** (1964) 1228]

[2] C W J Beenakker and H van Houten, Solid State Phys **44** (1991) 1

[3] C J Lambert, J Phys Condens Matter **5** (1993) 707

[4] C J Lambert, V C Hui, and S J Robinson, J Phys Condens Matter **5** (1993) 4187

[5] V T Petrashov, V N Antonov, P Delsing, and T Claeson, Phys Rev Lett **70** (1993) 347

[6] T M Klapwijk, Physica B **197** (1994) 481

[7] C W J Beenakker, Phys Rev Lett **67** (1991) 3836, **68** (1992) 1442(E)

[8] C W J Beenakker, in *Transport Phenomena in Mesoscopic Systems*, H Fukuyama and T Ando, eds (Springer, Berlin, 1992)

[9] The contribution of scattering inside the superconductor to the resistance of an NS junction has been studied extensively, see for example A B Pippard, J G Shepherd, and D A Tindall Proc R Soc London A **324** (1971) 17, A Schmid and G Schon, J Low Temp Phys **20** (1975) 207 T Y Hsiang and J Clarke, Phys Rev B **21** (1980) 945

[10] P G de Gennes, *Superconductivity of Metals and Alloys* (Benjamin, New York, 1966)

[11] K K Likharev, Rev Mod Phys **51** (1979) 101

[12] G E Blonder, M Tinkham, and T M Klapwijk, Phys Rev B **25** (1982) 4515

[13] C J Lambert, J Phys Condens Matter **3** (1991) 6579

[14] Y Takane and H Ebisawa, J Phys Soc Jpn **61** (1992) 1685

[15] C W J Beenakker, Phys Rev B **46** (1992) 12841

[16] A L Shelankov, Fiz Tverd Tela **26** (1984) 1615 [Sov Phys Solid State **26** (1984) 981]

[17] A V Zaïtsev, Zh Eksp Teor Fiz **86** (1984) 1742 [Sov Phys JETP **59** (1984) 1742]

[18] H van Houten and C W J Beenakker, Physica B **175** (1991) 187

[19] A V Zaïtsev, Zh Eksp Teor Fiz **78** (1980) 221, **79** (1980) 2016(E) [Sov Phys JETP **51** (1980) 111, **52** (1980) 1018(E)]

[20] M Buttiker, Phys Rev B **41** (1990) 7906

[21] M Buttiker, IBM J Res Dev **32** (1988) 63

[22] L I Glazman and K A Matveev, Pis'ma Zh Eksp Teor Fiz **49** (1989) 570 [JETP Lett **49** (1989) 659]

[23] C W J Beenakker and H van Houten, in *Single Electron Tunneling and Mesoscopic Devices*, H Koch and H Lubbig, eds (Springer, Berlin, 1992)

[24] V A Khlus, A V Dyomin, and A L Zazunov, Physica C **214** (1993) 413

[25] I A Devyatov and M Yu Kupriyanov, Pis'ma Zh Eksp Teor Fiz **52** (1990) 929 [JETP Lett **52** (1990) 311]

[26] F W J Hekking, L I Glazman, K A Matveev, and R I Shekhter, Phys Rev Lett **70** (1993) 4138

[27] O N Dorokhov, Solid State Comm **51** (1984) 381

[28] Y Imry, Europhys Lett **1** (1986) 249

[29] J B Pendry, A MacKinnon, and P J Roberts, Proc R Soc London A **437** (1992) 67

[30] Yu V Nazarov, Phys Rev Lett **73** (1994) 134

[31] A F Andreev, Zh Eksp Teor Fiz **51** (1966) 1510 [Sov Phys JETP **24** (1967) 1019]

[32] S N Artemenko, A F Volkov, and A V Zaïtsev, Solid State Comm **30** (1979) 771

[33] Y Takane and H Ebisawa, J Phys Soc Jpn **61** (1992) 2858

[34] A D Stone, P A Mello, K A Muttalib, and J -L Pichard, in *Mesoscopic Phenomena in Solids*, B L Al'tshuler, P A Lee, and R A Webb, eds (North Holland, Amsterdam, 1991)

[35] P A Mello and A D Stone, Phys Rev B **44** (1991) 3559

[36] C W J Beenakker, Phys Rev B **49** (1994) 2205

[37] A M S Macêdo and J T Chalker, Phys Rev B **49** (1994) 4695

[38] Y Takane and H Otani [J Phys Soc Jpn **63** (1994) 3361] find $\delta G_{NS} = \frac{4}{3} e^2/h$, in slight disagreement with eq (4 6)

[39] I K Marmorkos, C W J Beenakker, and R A Jalabert, Phys Rev B **48** (1993) 2811

[40] K -M H Lenssen, P C A Jeekel, C J P M Harmans, J E Mooij, M R Leys, J H Wolter, and M C Holland, in *Coulomb and Interference Effects in Small Electronic Structures*, D C Glattli and M Sanquer, eds (Editions Frontieres, Gif sur-Yvette, 1994)

[41] A Kastalsky, A W Kleinsasser, L H Greene, R Bhat, F P Milliken, and J P Harbison, Phys Rev Lett **67** (1991) 3026

[42] C Nguyen, H Kroemer, and E L Hu, Phys Rev Lett **69** (1992) 2847

[43] R G Mani, L Ghenim, and T N Theis, Phys Rev B **45** (1992) 12098

[44] N Agrait, J G Rodrigo, and S Vieira, Phys Rev B **46** (1992) 5814

[45] P Xiong, G Xiao, and R B Laibowitz, Phys Rev Lett **71** (1993) 1907

[46] K -M H Lenssen, L A Westerling, P C A Jeekel, C J P M Harmans, J E Mooij, M R Leys, W van der Vleuten, J H Wolter, and S P Beaumont, Physica B **194–196** (1994) 2413

[47] S J M Bakker, E van der Drift, T M Klapwijk, H M Jaeger, and S Radelaar, Phys Rev B **49** (1994) 13275

[48] P H C Magnee, N van der Post, P H M Kooistra, B J van Wees, and T M Klapwijk, Phys Rev B **50** (1994) 4594

[49] Y Takane and H Ebisawa J Phys Soc Jpn **62** (1993) 1844

[50] B J van Wees, P de Vries, P Magnee, and T M Klapwijk, Phys Rev Lett **69** (1992) 510

[51] Y Takane and H Ebisawa, J Phys Soc Jpn **61** (1992) 3466

[52] A F Volkov, A V Zaitsev, and T M Klapwijk, Physica C **210** (1993) 21

[53] F W J Hekking and Yu V Nazarov, Phys Rev Lett **71** (1993) 1625, Phys Rev B **49** (1994) 6847

[54] C W J Beenakker, B Rejaei, and J A Melsen, Phys Rev Lett **72** (1994) 2470

[55] A V Zaitsev, Pis'ma Zh Eksp Teor Fiz **51** (1990) 35 [JETP Lett **51** (1990) 41], Physica C **185–189** (1991) 2539

[56] A F Volkov and T M Klapwijk, Phys Lett A **168** (1992) 217

[57] A F Volkov, Pis'ma Zh Eksp Teor Fiz **55** (1992) 713 [JETP Lett **55** (1992) 746], Phys Lett A **174** (1993) 144

[58] A L Shelankov, Pis'ma Zh Eksp Teor Fiz **32** (1980) 122 [JETP Lett **32** (1980) 111]

[59] P A Mello and J -L Pichard, Phys Rev B **40** (1989) 5276

[60] O N Dorokhov, Pis'ma Zh Eksp Teor Fiz **36** (1982) 259 [JETP Lett **36** (1982) 318]

[61] P A Mello, P Pereyra, and N Kumar, Ann Phys **181** (1988) 290

[62] J A Melsen and C W J Beenakker, Physica B **203** (1994) 219

[63] D R Heslinga, S E Shafranjuk, H van Kempen, and T M Klapwijk, Phys Rev B **49** (1994) 10484

[64] A F Volkov, Phys Lett A **187** (1994) 404

[65] Yu V Nazarov Phys Rev Lett **73** (1994) 1420

[66] A I Larkin and Yu N Ovchinnikov, Zh Eksp Teor Fiz **68** (1975) 1915, **73** (1977) 299 [Sov Phys JETP **41** (1975) 960, **46** (1977) 155]

[67] M Yu Kupriyanov and V F Lukichev, Zh Eksp Teor Fiz **94** (1988) 139 [Sov Phys JETP **67** (1988) 1163]

[68] Yu V Nazarov, contribution at the NATO Adv Res Workshop on "Mesoscopic Superconductivity" (Karlsruhe, May 1994)

[69] H Pothier, S Guéron, D Esteve, and M H Devoret, Phys Rev Lett **73** (1994) 2488

[70] B Z Spivak and D E Khmel'nitskii, Pis'ma Zh Eksp Teor Fiz **35** (1982) 334 [JETP Lett **35** (1982) 412]

[71] B L Al'tshuler and B Z Spivak, Zh Eksp Teor Fiz **92** (1987) 609 [Sov Phys JETP **65**

      (1987) 343]
[72] H Nakano and H Takayanagi, Solid State Comm **80** (1991) 997
[73] S Takagi, Solid State Comm **81** (1992) 579
[74] C J Lambert, J Phys Condens Matter **5** (1993) 707
[75] V C Hui and C J Lambert, Europhys Lett **23** (1993) 203
[76] C W J Beenakker, Phys Rev Lett **70** (1993) 1155, Phys Rev B **47** (1993) 15763
[77] C W J Beenakker and B Rejaei, Phys Rev Lett **71** (1993) 3689, Phys Rev B **49** (1994) 7499
[78] J T Chalker and A M S Macêdo, Phys Rev Lett **71** (1993) 3693
[79] Y Takane and H Ebisawa, J Phys Soc Jpn **60** (1991) 3130
[80] J Bruun, V C Hui, and C J Lambert, Phys Rev B **49** (1994) 4010
[81] M J M de Jong and C W J Beenakker, Phys Rev B **49** (1994) 16070
[82] M Buttiker, Phys Rev Lett **65** (1990) 2901, Phys Rev B **46** (1992) 12485
[83] V A Khlus, Zh Eksp Teor Fiz **93** (1987) 2179 [Sov Phys JETP **66** (1987) 1243]
[84] G B Lesovik, Pis'ma Zh Eksp Teor Fiz **49** (1989) 513 [JETP Lett **49** (1989) 592]
[85] C W J Beenakker and M Buttiker, Phys Rev B **46** (1992) 1889
[86] K E Nagaev, Phys Lett A **169** (1992) 103
[87] B A Muzykantskii and D E Khmel'nitskii, Physica B **203** (1994) 238
[88] M J M de Jong and C W J Beenakker, Phys Rev B **46** (1992) 13400